

Measurement modelling of the International Reference System (SIR) for gamma emitting



**Bureau International
des Poids et Mesures**

1st edition 2007

Copyright statement

This document is distributed under the terms of the Creative Commons Attribution 4.0 International License (<http://creativecommons.org/licenses/by/4.0/>), which permits unrestricted use, distribution, and reproduction in any medium, provided you give appropriate credit to the original author(s) and the source, provide a link to the Creative Commons license, and indicate if changes were made.

Abstract

The photon and electron efficiency curves of an ionization chamber, as part of the SIR (International Reference System for activity measurements of γ -ray emitting radionuclides), have historically been determined using an iterative approach. That approach accounts for the influence of γ -ray-emitting impurities on the SIR measurement data based on experimental knowledge of the contributing effects or using the efficiency curves during the iterative process. Extrapolation of the curves is needed at the ends of the energy range to cover all photon and electron energies of interest.

The approach described here is based on a model that at the outset accounts for all available information, including impurity corrections and beta spectrum shapes. It also accounts for the uncertainties and known correlations associated with the SIR measurement data, the nuclear reference data and other effects. The only empirical parts of the model are the mathematical forms selected for the efficiency curves. Rather than using conventional functions such as polynomials, the approach works with the exponentials of polynomials. These forms are capable of exhibiting physically possible behaviour throughout the energy range, even though there is relatively sparse radionuclide data available at high energies.

Rather than correcting the measurement data for impurities, as is conventional in this area, the model itself is adjusted. The benefit of this approach is that the polynomial coefficients can be determined using generalized non-linear least-squares minimization. The adjusted model matches the SIR measurement data as closely as possible, taking account of the uncertainties and correlations indicated above. Although the solution to this least-squares formulation requires iterative solution algorithmically, it is not iterative in the sense of previous methods.

This process provides estimates of the efficiency values of the ionization chamber, and the associated uncertainties, at any photon or electron energy. The uncertainties associated with the response of the ionization chamber for all radionuclides of interest are also evaluated.

Measurement modelling of the International Reference System (SIR) for gamma emitting radionuclides Contents

Foreword	8
Executive summary	9
1. Introduction and overview of approach	10
1.1. General	10
1.2. Overview of approach	12
2. Input data, associated uncertainties and data corrections	15
2.1. Equivalent activity measurement data	15
2.2. Data relating to relative impurity activities	17
2.3. Nuclear reference data	17
2.4. Key comparison reference values	18
3. Model building	20
3.1. Generic form for the efficiency function of the ionization chamber	20
3.2. Representation of the photon and electron efficiency functions	20
3.3. Accounting for impurity corrections	23
4. Solution characterization	24
4.1. Matching modelled and measured values	24
4.2. Measure of deviation of model from data	25
4.3. Equation characterizing the solution	26
5. Model parameter determination	28
5.1. General	28
5.2. First-order derivative evaluation	28
5.3. Use of a generalized non-linear least-squares solver	28
5.4. Initial approximations to the model parameters	29
6. Model parameter uncertainties	30
6.1. General	30
6.2. Implicit model	30
7. Validation of model and uncertainty evaluation	32
7.1. Choice of models from model families	32
7.2. Consistency of model and data	33
7.3. Determining a consistent subset	33
7.4. Uncertainty check by Monte Carlo calculation	34

7.5. Adequacy of quadrature rule	34
8. Determination of the required quantities and the associated uncertainty evaluation	36
8.1. Parameters of the photon and electron efficiency curves	36
8.2. Corrected measured equivalent activity	36
8.3. Modelled equivalent activity	37
9. Summary of computational procedure	38
10. Results	40
10.1. Application of the procedure to the SIR	40
10.2. Application of the procedure to other ionization chambers	46
11. Conclusions	48
11.1. Problem formulation	48
11.2. Problem solution	48
11.3. Scope for further work	48
References	62
Appendix 1. Glossary	50
Appendix 2. Derivatives required by the generalized non-linear least-squares algorithm and in the evaluation of uncertainties	56
Appendix 3. Hessian matrices	59
Appendix 4. Implicit multivariate model	60

Foreword

This monograph is one of a series published by the Bureau International des Poids et Mesures (BIPM) on behalf of the *Comité Consultatif des Rayonnements Ionisants* (CCRI). The aim of this series of publications is to review topics that are of importance for the measurement of ionizing radiation and especially of radioactivity, in particular those techniques normally used by participants in international comparisons. It is hoped that these publications will prove to be useful reference volumes both for those who are already engaged in this field and for those who are approaching such measurements for the first time.

The purpose of this monograph, number 7 in the series, is to present a mathematically compact and elegant way of modelling the photon and electron efficiency curves of ionization chambers, developed specifically for the International Reference System for gamma-ray activity comparisons (SIR). Corrections for impurities are taken into account in a manner that is consistent with the modelling of the photon and electron response of the chamber. A comprehensive scheme for determining the uncertainties is provided. The model also provides reliable and robust values for radionuclides measured in the SIR for the first time.

Although the computer code has been developed for the SIR, the method is generally applicable to all well-type ionization chambers. Consequently, the computer code will be made available to National Metrology Institutes together with a protocol to explain its detailed application.

G. Moscati
President of the CCRI

A.J. Wallard
Director of the BIPM

Executive summary

1. The SIR ionization chamber at the BIPM is used to establish equivalence of radioactivity measurements made by the national metrology institutes (NMIs) of the signatory members of the Metre Convention.
2. To this end each NMI submits to the BIPM samples of solutions of radionuclides and their measured values of the activity of these solutions. Each NMI also provides information on any radionuclidic impurities that may be present. The BIPM measures these samples in the ionization chamber, comparing the current produced with that produced by a radium reference source.
3. The so-called equivalent activity is derived from the ratio of the currents and the NMI-supplied activity, with corrections for radioactive decay and impurities.
4. The correction for impurities requires that any impurities present have previously been measured and their equivalent activities known. Unfortunately this knowledge is frequently not available. A model is therefore required to predict the responses for such radionuclides.
5. The ionization chamber efficiency curves are modelled empirically by exponentials of polynomials, the polynomial coefficients being determined by a generalized non-linear least-squares fit. The least-squares procedure takes as input the photon and electron emission spectra and known equivalent activities and produces as output the best estimate of the polynomial coefficients for the efficiency curves.
6. The photon emission spectra are generally well known and there is evaluated and published data of good quality for most of the radionuclides of interest. However, the beta spectra are less well known (being considerably more difficult to measure) and a calculation from first principles is required.
7. The radionuclides ^{177}Lu , ^{182}Ta and ^{99}Mo are used as test cases following the least-squares fit. The model successfully predicts equivalent activities for these radionuclides.
8. By comparing modelled and measured equivalent activities it is possible to identify radionuclides for which there may be inconsistencies in the published photon emission data. This is the case for ^{201}Tl and ^{65}Zn [32].

1. Introduction and overview of approach

1.1. General

The SIR (International Reference System for activity measurements of γ -ray emitting radionuclides) was established in 1976 at the Bureau International des Poids et Mesures (BIPM) to complement the international comparisons of activity measurements organized by Section II of the CCRI (Comité Consultatif des Rayonnements Ionizants). Participating laboratories submit SIR glass ampoules containing their standardized solutions of radionuclides to the BIPM, where the current produced by these samples in a 4π -ionization well chamber (ionization chamber) is compared with the current obtained with a ^{226}Ra reference source [40]. The simplicity and rapidity of the measurement as well as the long-term stability of the ionization chamber has allowed the comparison over 30 years of hundreds of radioactive solutions for a total of about 60 radionuclides.

Some of the radionuclides considered are also beta emitters. The consequent *bremsstrahlung* (radiation emitted by charged particles under deceleration) produced mainly in the wall of the ionization chamber contributes to the measured ionization current and must be taken into account.

The detection efficiency of the SIR ionization chamber for a given photon of energy E or electron of energy W is the ionization current produced in the ionization chamber by a source emitting 10^3 such radiations per second, expressed relative to the ionization current produced in the ionization chamber by the BIPM ^{226}Ra reference source $I_{\text{Ra},5}$.

Similarly, the detection efficiency ε of the SIR ionization chamber for a given radionuclide is the ratio of (a) the ionization current I produced in the ionization chamber per activity A of that radionuclide measured by a laboratory in kBq and (b) the ionization current $I_{\text{Ra},5}$.

Efficiency curves (detection efficiency versus photon energy and detection efficiency versus electron energy) are required for the calculation of the response of the ionization chamber for radionuclides not previously measured in the SIR. They are needed to evaluate the correction for a photon-emitting impurity present in an ampoule when the efficiency for this impurity is not known experimentally [30], or to give a point of comparison when a radionuclide is measured in the SIR for the first time. Each SIR measurement can be considered as a determination of the efficiency of the ionization chamber for a given radionuclide [36], [38]. In consequence the whole set of SIR measurement data can be used, in principle, to establish the required efficiency curve.

However, in order to obtain reliable efficiency curves, a selection of the data is made: only the results based on NMI primary standardizations are used, which are those retained for the calculation of the key comparison reference values (KCRVs) of the CIPM MRA [7]. In addition, for physical reasons, gaseous radionuclides and strong β^+ emitters are excluded. Further, for low-energy photon emitters and strong β emitters, radioactive solutions of low acid and carrier concentrations are selected in order to minimize the influence of self-attenuation.

Since physical models for the efficiency curves are not available, previous methods have used empirical representations of these curves in the form of polynomials, exponentials, and products of polynomials and exponentials. The adjustable parameters (e.g., polynomial coefficients) in the representations are determined by iteration. This is to account for the influence of gamma-ray-emitting impurities and also to deal with the multi-photon emitters,

the efficiency for one photon being deduced from the measured equivalent activity by subtracting the contribution of all other photons as estimated from the previous iteration [31], [41], [42]. The iterative schemes have been based on a physical knowledge of the relative magnitudes of the contributory effects. Least-squares minimizations were also applied by several authors [23], [43], [44]. However, corrections for impurities were not included in the model equations and the associated uncertainty evaluation was not fully treated.

The approach considered here is different. A least-squares formulation is used that accounts for available physical information and measurement uncertainties (Chapter 3, see p. 20). The formulation, as in the above cited references, allows for the presence of radioactive impurities [30]. Families of empirical functions are used within this formulation to represent the efficiency curves (Section 3.2, see p. 20). Although as in previous approaches these functions are empirical in nature, they are chosen to take a form that ensures they are capable of possessing physically possible behaviour.

In the context of data modelling, the nature of the problem is unconventional. The measurement data would not be expected to lie on the desired model curve, even if it were possible to make each measurement perfectly and correct it precisely for the respective radioactive decays and any impurity content. Such a ‘perfectly adjusted’ measured value of a radionuclide in solution would only lie on the curve if it decayed by a single energy photon emission. The model curve is a continuous function of energy, whereas each radionuclide has a number of discrete energy emissions and so cannot be represented by a single energy.

The use of appropriate least-squares modelling principles permits a statistically valid solution to be obtained. Such a solution would not be obtainable were some of the data inconsistent with the model, for example as a consequence of an incorrectly recorded measured value or the stipulation of too small an uncertainty associated with a measured value. The approach *simultaneously* provides the required efficiency curves and corrects the measurements for impurities (Chapter 5, see p. 28).

The parameters of the empirical functions occur non-linearly within the overall model. Accordingly, recognized, high-quality algorithms for solving generalized non-linear least-squares problems are applied [2]. In particular, the uncertainties associated with the various physical quantities involved are properly taken into account [18].

The resulting efficiency functions enable efficiency values to be provided for any radionuclide with known nuclear reference data, *whether previously measured in the SIR or not*, together with the associated uncertainties.

Validation procedures (Chapter 7, see p. 32) (a) permit the selection of appropriate members of the families of empirical functions considered, (b) check the adequacy of the numerical quadrature rule used when evaluating the model, © provide an assessment of the consistency of the model and the data and the uncertainties associated with the data, and (d) consider the physical feasibility of the computed model.

The formulation caters for the uncertainties associated with the measured values of radionuclide activity provided by the laboratories. The uncertainties associated with the estimates of the model parameters can be formed from the information provided by the algorithm used to solve the generalized non-linear least-squares problem. In turn, these uncertainties are propagated through the models for a given energy to obtain the uncertainties associated with the corresponding efficiency values. There are further uncertainty sources that are taken into account and that influence the uncertainties associated with these efficiency values. These sources relate to the tabular values of the nuclear reference data used in the

model for photon and beta-transition energies and the corresponding probabilities. They also relate to the relative impurity activities. The uncertainties associated with these sources are propagated through the model, and combined with the above-mentioned uncertainties.

In this work, a distinction is made between (a) quantities themselves and (b) estimates of quantities or data values of quantities. Quantities are regarded as random variables in that they are not known exactly. Knowledge of a quantity is characterized by a probability distribution. A best estimate of that quantity is then the expectation of that quantity so characterized, and the standard uncertainty associated with that estimate is the standard deviation of the quantity. An example of a quantity is a parameter in a model, such as the gradient of a straight-line calibration function. An estimate of that quantity would generally be obtained by fitting that function to calibration data. Another example of a quantity is the emission probability of a photon. A data value of the quantity would be provided in nuclear reference data tables. These considerations are consistent with those of the GUM [9].

Appendix 1 contains a glossary of symbols used.

A distillation of the detailed exposition here is available [32], [36].

1.2. Overview of approach

The starting point of the approach is the consideration of the data that is available relating to the problem of concern and the physical quantities of which this data constitutes particular values (section 2). There are four categories of data:

1. data vector $\hat{\mathbf{R}}$, regarded as a best estimate of \mathbf{R} , the vector representing the relative impurity activities (Section 2.2, see p. 17);
2. data vector $\hat{\mathbf{D}}$, regarded as a best estimate of \mathbf{D} , the vector of equivalent activity measurement quantities for the radionuclides and laboratories of concern (Section 2.1, see p. 15);
3. data vector $\hat{\mathbf{N}}$, regarded as a best estimate of \mathbf{N} , the vector representing nuclear reference data quantities (Section 2.3, see p. 17);
4. data vector $\hat{\mathbf{K}}$, regarded as a best estimate of \mathbf{K} , the vector representing those KCRVs available for the radionuclides of concern (Section 2.4, see p. 18).

Associated with each of these data vectors is an uncertainty matrix (covariance matrix).

The uncertainty matrix associated with $\hat{\mathbf{R}}$ is denoted by $\mathbf{V}_{\hat{\mathbf{R}}}$, with a similar notation for the other uncertainty matrices. Mostly, these uncertainty matrices are diagonal, with the diagonal elements containing the squares of the standard uncertainties associated with the individual data items or estimates. When a covariance associated with a pair of data items, the i th and j th, say, is available, it is included as elements (i, j) and (j, i) of the corresponding uncertainty matrix.

Account is not taken here of the uncertainties associated with the elements of $\hat{\mathbf{K}}$, since their influence compared with those of $\hat{\mathbf{D}}$, $\hat{\mathbf{N}}$ and $\hat{\mathbf{R}}$ would be expected to be small. See Chapter 11.

It is necessary to incorporate correction factors that compensate for the fact that a solution containing a particular radionuclide measured by a laboratory may contain impurities (Section

2.1, see p. 15). Such correction is not necessarily purely numerical because in general it depends on the vector \mathbf{B} of parameters of the efficiency curves that is to be determined and also on \mathbf{R} and \mathbf{N} . The manner in which this aspect is handled is covered in the approach used for the modelling (Section 3.3, see p. 23).

An established generic form for the model [31] for the efficiency (the reciprocal of equivalent activity) ε_i of the ionization chamber for radionuclide i is used (Section 3.1, see p. 20). Letting E denote photon energy and W electron energy, this model is expressed in terms of the photon efficiency function $\varepsilon(E)$ and the electron efficiency function $\varepsilon_\beta(W)$. Since functional forms for the photon and electron efficiency functions are not available from physical considerations, they are modelled empirically in terms of appropriate functions involving unknown parameter vectors $\mathbf{B}^{(1)}$ and $\mathbf{B}^{(2)}$, respectively, constituting the (combined) parameter vector \mathbf{B} (Section 3.2.1, see p. 20).

The empirical modelling functions used are transformed polynomial functions having the properties that they exhibit physically possible behaviour, namely they are positive for all energy values and they tend to zero at low energy. To ensure numerical stability of the consequent computation, these polynomials are expressed in Chebyshev form (Section 3.2.2, see p. 22).

To account for impurities, a functional form for impurity correction based on the considerations of Section 2.1 is used that depends on \mathbf{B} , \mathbf{N} and \mathbf{R} (Section 3.3, see p. 23). This form is generalized through the use of a mixing ratio to reflect the use of previously evaluated but not totally reliable equivalent activity values. This use also results in a simplification of the formulae subsequently required in the uncertainty evaluation.

In order to estimate the parameter vector \mathbf{B} , an appropriate measure of match of modelled and measured values of equivalent activity is minimized. A measure based directly on the considerations so far would give rise to an unconventional formulation because of the dependence of the ‘measured’ equivalent activities on \mathbf{B} through the modelled correction for impurities. It is shown, however (Section 4.1, see p. 24), that a simple transformation of the problem results in a formulation in conventional form, in which a model consisting of the quotient of modelled equivalent activity and impurity correction factor is matched to \mathbf{D} . The resulting measure is discussed (Section 4.2.1, see p. 25) in the context of a formulation that incorporates the given uncertainty information. Minimization of this measure constitutes solving a *generalized non-linear least-squares problem*.

In the full formulation of this problem, \mathbf{D} , \mathbf{B} , \mathbf{N} and \mathbf{R} are estimated to provide *posterior estimates* given *prior estimates* $\hat{\mathbf{D}}$ (laboratories’ measured equivalent activity values not corrected for impurities), $\hat{\mathbf{B}}$ (e.g. from previous work on determining efficiency curves), $\hat{\mathbf{N}}$ (published nuclear reference data), and $\hat{\mathbf{R}}$ (relative impurity activity data). Any evidence of a mis-match of posterior and prior estimates could be used to propose a consequent adjustment to the nuclear data but in practice would be used to focus the radionuclide community on making appropriate investigations. Moreover, this full formulation, although appropriate for the problem, gives rise to computational difficulties because of the large number of quantities and hence the large matrices involved. Instead, therefore, a partial formulation is given that avoids these difficulties, which has good rather than near-optimal statistical properties (Section 4.2.2, see p. 26). All quantities are fixed at their prior estimates apart from the curve parameters \mathbf{B} . Solution of this formulation also constitutes solving a *generalized non-linear least-squares problem*, but of much smaller size. Although they are not needed in solving this least-squares problem, equations characterizing the resulting solution

(Section 4.3, see p. 26) are given. They are required subsequently in order to evaluate the uncertainty matrix associated with the estimate \mathbf{B}^* of \mathbf{B} (Chapter 6, see p. 30).

The algorithm recommended for solving generalized non-linear least-squares problems is iterative in nature, at each iteration producing what is generally an improved approximation to the solution. For each approximation to \mathbf{B}^* , the algorithm requires the values of the partial derivatives of first order of the impurity-corrected equivalent activity model. Expressions are derived for these derivatives (Section 5.2 and Appendix 2, see p. 56). The use of a generalized non-linear least-squares solver (Section 5.3, see p. 28) and the determination of initial approximations to the model parameters (Section 5.4, see p. 29), required for iterative solution, are considered.

Were the solution of the full formulation feasible, the uncertainty matrix $\mathbf{V}_{\mathbf{B}^*}$ associated with the estimate \mathbf{B}^* of the model parameter vector \mathbf{B} would be available as a by-product of the least-squares procedure. This uncertainty matrix would reflect the uncertainties associated with $\hat{\mathbf{D}}$, $\hat{\mathbf{N}}$ and $\hat{\mathbf{R}}$. For the partial formulation, the $\mathbf{V}_{\mathbf{B}^*}$ provided would account only for the uncertainties associated with $\hat{\mathbf{D}}$, and take the form [29]

$$\mathbf{V}_{\mathbf{B}^*} = \left(\mathbf{J}_s^T(\mathbf{B}) \mathbf{V}_{\hat{\mathbf{D}}}^{-1} \mathbf{J}_s(\mathbf{B}) \right)^{-1},$$

where $\mathbf{J}_s(\mathbf{B})$ is the (Jacobian) matrix containing the partial derivatives of first order of the model residual deviations \mathbf{s} with respect to the model parameters.

The further sources of uncertainty to be taken into account, associated with the estimates $\hat{\mathbf{N}}$ of \mathbf{N} and $\hat{\mathbf{R}}$ of \mathbf{R} , are propagated through the least-squares solution, to be combined with the above-mentioned uncertainties. These further uncertainties are taken into account using a generalization of the GUM uncertainty framework.

The solution obtained as described corresponds to the use of estimates regarded as the expectations of distributions for the corresponding quantities. On the basis of the principles of GUM Supplement 1 [8], such distributions would be assigned to be Gaussian with expectations equal to the estimates and standard deviations equal to the standard uncertainties associated with these estimates.

At the solution to the generalized non-linear least-squares problem, the partial derivatives with respect to the adjustable quantities \mathbf{B} are zero. The resulting expressions provide a measurement model relating input quantities \mathbf{D} , \mathbf{R} and \mathbf{N} to output quantities \mathbf{B} that can be used as the basis for applying the GUM uncertainty framework. In terms of a classification of measurement models [19], this model is categorized as (a) *multivariate* (having a number of output quantities), (b) *implicit* (being defined in such a way that \mathbf{B} cannot be expressed directly in terms of \mathbf{D} , \mathbf{R} and \mathbf{N}), and © *real* (not involving complex quantities).

2. Input data, associated uncertainties and data corrections

This section discusses the various data items and the quantities of which these data items constitute realizations that are used in the modelling, namely those indicated in Section 1.2, 1)-Section 1.2, 4). It also considers the available uncertainties associated with these data items. It further considers the correction factors that compensate for the presence of impurities in the radioactive solutions.

2.1. Equivalent activity measurement data

Equivalent activity measurement data are derived from more fundamental measurement data. Consider an SIR measurement of a radioactive solution, in a glass ampoule, containing a radionuclide, generally with impurities. Let A denote the *activity* of the solution at a reference date t_r , that is when the measurement was made by a participating laboratory.

The *equivalent activity* A_e is the activity of the solution that would produce the same ionization current as the reference ^{226}Ra source number 5 at the fixed SIR reference date t_0 .

Let $I_{\text{Ra},s}$ and I denote the ionization currents produced by the ^{226}Ra source number s and the ampoule, respectively. Let I_f denote the background current. There will be a value for each of these three currents corresponding to each laboratory's measurement.

Let t_m be the date of the SIR measurement of the solution, and λ_{Ra} and λ_i the decay constants of ^{226}Ra and a measured radionuclide i , respectively.

Three multiplicative factors are used to transform A to A_e [30]:

1. The product of the quotient

$$\frac{I_{\text{Ra},s} - I_f}{I - I_f}$$

of the respective ionization currents, allowing for the background current, and a factor F_s that is the quotient of currents of radium source numbers 5 and s .

2. The decay-correction factor

$$\frac{\exp(-\lambda_i(t_m - t_r))}{\exp(-\lambda_{\text{Ra}}(t_m - t_0))}$$

due to the respective decay constants and the times elapsed to the date of the SIR measurement.⁽¹⁾

3. An impurity correction factor C that accounts for the impurities in the solution.

Thus [30],

$$A_e = AMC, \quad (1)$$

where

$$M = F_s \frac{I_{\text{Ra},s} - I_f}{I - I_f} \frac{\exp(-\lambda(t_m - t_r))}{\exp(-\lambda_{\text{Ra}}(t_m - t_0))}$$

⁽¹⁾ This factor is not applicable to short-lived radionuclides for which the decay is significant during measurement and the decay correction is evaluated by integrating the numerator over measurement time.

and C is considered below. The A and M are combined to form the current- and decay-corrected measurement quantity

$$D = AM = AF_s \frac{I_{\text{Ra},s} - I_f}{I - I_f} \frac{\exp(-\lambda(t_m - t_f))}{\exp(-\lambda_{\text{Ra}}(t_m - t_0))}.$$

Equation (1) corresponds to the equivalent activity *per se* that is current-, decay- and impurity-corrected.

The above notation is qualified as follows when a measurement is made of radionuclide i by a laboratory (indexed by) ℓ :

$$(A_e)_{i,\ell}^{\text{meas}} = D_{i,\ell} C_{i,\ell}, \quad (2)$$

where

$$D_{i,\ell} = A_{i,\ell} M_{i,\ell}. \quad (3)$$

The superscript in $(A_e)_{i,\ell}^{\text{meas}}$ is used to emphasize that equivalent activity is based on *measurement*. (Subsequently, another superscript will indicate when equivalent activity is based on a *model*.) The $A_{i,\ell}$ denotes the measured value for the activity of radionuclide i provided by laboratory ℓ . The $M_{i,\ell}$ denotes the value of M in Equation (1) relevant to radionuclide i and laboratory ℓ , namely,

$$M_{i,\ell} = F_s \frac{(I_{\text{Ra},s})_{i,\ell} - (I_f)_{i,\ell}}{I_{i,\ell} - (I_f)_{i,\ell}} \frac{\exp(-\lambda_i((t_m)_{i,\ell} - (t_f)_{i,\ell}))}{\exp(-\lambda_{\text{Ra}}((t_m)_{i,\ell} - t_0))}. \quad (4)$$

The $C_{i,\ell}$ is the correction factor that compensates for the fact that the solution containing radionuclide i that is measured by laboratory ℓ may contain impurities, and is given [30] by

$$C_{i,\ell} = 1 + \sum_{k \in K_{i,\ell}} R_{i,\ell,k} \frac{(A_e)_i}{(A_e)_k} \quad (5)$$

(see Section 2.2, see p. 17).

Let \mathbf{D} denote the vector of values of the $D_{i,\ell}$. It constitutes the set of current- and decay-corrected measurement quantities, or in brief the *data quantity vector*.

The modelling approach described here utilizes the $D_{i,\ell}$ and therefore requires the standard uncertainties $u(\hat{D}_{i,\ell})$ associated with estimates $\hat{D}_{i,\ell}$ of the $D_{i,\ell}$ given by

$$\hat{D}_{i,\ell} = \hat{A}_{i,\ell} \hat{M}_{i,\ell},$$

using Equation (3), where $\hat{A}_{i,\ell}$ is the measured value provided by laboratory ℓ of the activity of radionuclide i and $\hat{M}_{i,\ell}$ is the value of $M_{i,\ell}$ given by substituting measured values for the various quantities in the right-hand side of Equation (4).

These uncertainties are given by applying the law of propagation of uncertainty to Equation (3), under the assumption that the quantities involved are mutually independent, to give

$$\frac{u^2(\hat{D}_{i,\ell})}{\hat{D}_{i,\ell}^2} = \frac{u^2(\hat{A}_{i,\ell})}{\hat{A}_{i,\ell}^2} + \frac{u^2(\hat{M}_{i,\ell})}{\hat{M}_{i,\ell}^2}, \quad (6)$$

where $u(\hat{A}_{i,\ell})$ is the standard uncertainty associated with $\hat{A}_{i,\ell}$ as declared by laboratory ℓ , and $u(\hat{M}_{i,\ell})$ that associated with $\hat{M}_{i,\ell}$. The $u(\hat{M}_{i,\ell})$ is obtained by applying the law of propagation of uncertainty to Equation (4), given the standard uncertainties associated with the measured values of the quantities involved.

Generally the $C_{i,\ell}$ in Equation (5) will depend on the model parameters \mathbf{B} , say, which are to be determined. They also depend on \mathbf{N} and \mathbf{R} , estimates of which, with associated standard uncertainties, are available (see Section 3.3, see p. 23).

2.2. Data relating to relative impurity activities

Consider the activity ratio quantities $\tilde{R}_{i,\ell,k}$, $k \in K_{i,\ell}$ corresponding to the activities at the reference date of impurity k in a solution of radionuclide i for laboratory ℓ , for all relevant i , ℓ and k . The $K_{i,\ell}$ denotes the index set relating to impurities associated with that solution. Let \mathbf{R} denote the vector of decay-corrected quantities $R_{i,\ell,k}$ for relevant i , ℓ and k . Data constituting a best estimate $\hat{\mathbf{R}}$ of \mathbf{R} is available, as are the associated standard uncertainties.

The $R_{i,\ell,k}$ is given by

$$R_{i,\ell,k} = \tilde{R}_{i,\ell,k} H_{i,\ell,k},$$

where

$$H_{i,\ell,k} = \exp\left(-(\lambda_k - \lambda_i)\left((t_m)_{i,\ell} - (t_r)_{i,\ell}\right)\right)$$

is the appropriate decay correction.

Consider the correction factors $C_{i,\ell}$ in Equation (5). The value provided by laboratory ℓ in its measurement of a solution containing radionuclide i will fall into one of three categories, corresponding to the measurement of a radionuclide

1. that is pure, in which case $C_{i,\ell} = 1$,
2. together with impurities that have all previously been well characterized in terms of reliable measurement, meaning that KCRVs for the equivalent activities $(A_e)_i$ and $(A_e)_k$ in Equation (5) would be available, and hence a numerical value for $C_{i,\ell}$ could be determined, and
3. together with impurities not all of which have previously been well characterized. For the well-characterized impurities, KCRVs for the $(A_e)_k$ in Equation (5) would again be available, but the efficiency model is used to estimate the remaining impurities.

2.3. Nuclear reference data

For a radionuclide (indexed by) i let

- J_i denote the set of indices of the photons associated with this radionuclide,
 βJ_i the set of indices of the beta transitions associated with this radionuclide,

⁽¹⁾ The ‘emission probability’ $P_{i,j}$ of a given particle or photon is the mean number of such particles or photons emitted per decay. For β^\pm and

$E_{i,j}$	the energy associated with the j th photon,
$P_{i,j}$	the emission probability for the j th photon ⁽¹⁾ ,
$W_{i,j}$	the maximum energy associated with the j th beta-transition,
${}_{\beta}P_{i,j}$	the emission probability for the j th beta-transition,
$S_{i,j}(W)$	the energy distribution function for the spectrum corresponding to the j th beta-transition, normalized such that

$$\int_1^{\infty} S_{i,j}(W) dW = 1,$$

where $W = E/(m_e c^2) + 1$ is the reduced total electron energy, m_e being the rest mass of the electron and c the speed of light.

Values of the quantities $\{E_{i,j}: j \in J_i\}$, $\{P_{i,j}: j \in J_i\}$, $\{W_{i,j}: j \in {}_{\beta}J_i\}$ and $\{{}_{\beta}P_{i,j}: j \in {}_{\beta}J_i\}$ are available as published *nuclear reference data*, together with associated standard uncertainties (see e.g. [4], see p. 62). These published energies and probabilities are regarded as best-available estimates $\hat{\mathbf{N}}$ of quantities collectively labelled \mathbf{N} . In general, only a subset of the nuclear reference data is used and \mathbf{N} and $\hat{\mathbf{N}}$ are interpreted accordingly.

For the problem here most of the quantities concerned are independent and hence $\mathbf{V}_{\hat{\mathbf{N}}}$ is predominantly diagonal. However, there are some correlation effects associated with (a) the nuclear reference data relating to the normalization of the relative emission probabilities⁽²⁾, and (b) an emission probability in the case where two laboratories provide activity estimates having small associated uncertainties. The $\mathbf{V}_{\hat{\mathbf{N}}}$ will consequently contain some off-diagonal non-zero elements.

The beta energy distribution function $S_{i,j}$, for the j th beta transition, is calculated as in the publications of Wilkinson [45], [46], [47], [48], [49]. The first- and second-forbidden non-unique decays are approximated by allowed and first-forbidden unique decays, respectively. The required values of the Coulomb functions λ_n are approximated as independent of energy and estimated from the tables of Behrens and Jänecke [5]. The ‘finite nuclear radius’ is estimated by the relation given in Grau Malonda [28]. The electron shielding correction is calculated by the method of Rose [39], where the total positron/electron energy in the Fermi function is shifted by a screening potential $\pm V_s$.

The emission of conversion electrons of energy W_c is taken into account by defining a special case of energy distribution: $S_{i,j} = \delta(W - W_c)$.

γ emissions the $P_{i,j}$ are physically constrained to $0 \leq P_{i,j} \leq 1$ and equate to the probabilities of emission following decay. For X-rays or annihilation radiation there may be more than one photon emitted per decay and the $P_{i,j}$ no longer represent probabilities *per se*. However, the $P_{i,j}$ are conventionally referred to as ‘emission probabilities’ regardless of the physical process.

⁽²⁾ For a particular radionuclide i , the $P_{i,j}$ are obtained as $P_{i,j} = \eta_i I_{i,j}$, where $I_{i,j}$ is the relative emission probability for the j th photon for radionuclide i and η_i is a normalization factor for that radionuclide. Standard uncertainties are available for the η_i and the $I_{i,j}$. The $P_{i,j}$ so obtained are correlated. Specifically, applying the law of propagation of uncertainty, $u^2(P_{i,j}) = I_{i,j}^2 u^2(\eta_i) + \eta_i^2 u^2(I_{i,j})$ and $u(P_{i,j}, P_{i,j'}) = I_{i,j} I_{i,j'} u^2(\eta_i)$.

2.4. Key comparison reference values

Let $(A_e)_i^{\text{KCRV}}$ denote a key comparison reference value (KCRV) for radionuclide i . For many of the radionuclides, such a KCRV is published in the BIPM Key Comparison Database (KCDB) [6] and is considered to be a best estimate, together with an associated standard uncertainty, of the equivalent activity. The model may be used ultimately to derive KCRVs for other radionuclides [37]. The set of such KCRVs is denoted by $\hat{\mathbf{K}}$ and the vector of quantities of which $\hat{\mathbf{K}}$ is a realization is denoted by \mathbf{K} .

Account is not taken here of the uncertainties associated with the elements of $\hat{\mathbf{K}}$, since their influence compared with those of $\hat{\mathbf{D}}$, $\hat{\mathbf{N}}$ and $\hat{\mathbf{R}}$ would be expected to be small. See Chapter 11.

3. Model building

3.1. Generic form for the efficiency function of the ionization chamber

Denote by $\varepsilon(E)$ the efficiency of the ionization chamber for photons of energy E , and by $\varepsilon_\beta(W)$ its efficiency for electrons of energy W . The function $\varepsilon(E)$ is known as the *photon efficiency function or photon efficiency curve* and $\varepsilon_\beta(W)$ as the *electron efficiency function or curve*. Since analytical forms for these functions derived from *physical principles* are not available, $\varepsilon(E)$ is modelled by an appropriate *empirical* function $F(\mathbf{B}^{(1)}, E)$ and $\varepsilon_\beta(W)$ by $G(\mathbf{B}^{(2)}, W)$. The $\mathbf{B}^{(1)}$ and $\mathbf{B}^{(2)}$ denote sets of adjustable model parameters, with $\mathbf{B} = \left((\mathbf{B}^{(1)})^\top, (\mathbf{B}^{(2)})^\top \right)^\top$, that is

$$\mathbf{B} = \begin{bmatrix} \mathbf{B}^{(1)} \\ \mathbf{B}^{(2)} \end{bmatrix},$$

representing the aggregated set of adjustable model parameters.

The model for the efficiency of the chamber for radionuclide i is given [31] by

$$\varepsilon_i = \sum_{j \in J_i} P_{i,j} F(\mathbf{B}^{(1)}, E_{i,j}) + \sum_{j \in \beta J_i} P_{i,j} \int_1^{W_{i,j}} S_{i,j}(W) G(\mathbf{B}^{(2)}, W) dW. \quad (7)$$

The corresponding model for the equivalent activity [31], [38], [41] of radionuclide i , indicating explicitly that it depends on \mathbf{B} and \mathbf{N} , is

$$(A_e)_i^{\text{model}}(\mathbf{B}, \mathbf{N}) = \varepsilon_i^{-1} = \left[\sum_{j \in J_i} P_{i,j} F(\mathbf{B}^{(1)}, E_{i,j}) + \sum_{j \in \beta J_i} P_{i,j} \int_1^{W_{i,j}} S_{i,j}(W) G(\mathbf{B}^{(2)}, W) dW \right]^{-1}. \quad (8)$$

This quantity is the model value for the equivalent activity of radionuclide i .

3.2. Representation of the photon and electron efficiency functions

3.2.1. Physically possible empirical models

Although the *form* of the efficiency functions $F(\mathbf{B}^{(1)}, E)$ and $G(\mathbf{B}^{(2)}, W)$ is not known analytically, they are expected to vary smoothly with energy, reasons for which have been given [40]. Hence, appropriate smooth empirical functions containing adjustable parameters are required. Because of the arbitrariness of choice, it is important that the functions used are validated by confirming that there is no lack of consistency of model and data. This aspect is addressed in Chapter 7, and also mentioned later in this section.

Consider first models of the form

$$F(\mathbf{B}^{(1)}, E) = \sum_{h=1}^n B_h^{(1)} \phi_h(E), \quad (9)$$

$$G(\mathbf{B}^{(2)}, W) = \sum_{h=1}^{n\beta} B_h^{(2)} \psi_h(W),$$

where $(B^{(1)}, \dots, B_n^{(1)})$ are the elements of $\mathbf{B}^{(1)}$ and $(B_1^{(2)}, \dots, B_{n\beta}^{(2)})$ those of $\mathbf{B}^{(2)}$, and the $\phi_h(E)$ and $\psi_h(W)$ are suitable sets of basis functions. Possible basis functions are powers of E or W (making $F(\mathbf{B}^{(1)}, E)$ or $G(\mathbf{B}^{(2)}, W)$ a polynomial in E or W) and B-splines for a prescribed set of knots (making $F(\mathbf{B}^{(1)}, E)$ or $G(\mathbf{B}^{(2)}, W)$ a spline with these knots). Appropriately transformed polynomials were used for this application. A suitable representation of polynomials (Section 3.2.2, see p. 22) is used for numerical purposes.

Appropriate orders of the polynomials are required to ensure that the model is consistent with the data, accounting for the uncertainties. Generally, unless adequate data are available, a polynomial might exhibit oscillations in order to be ‘close’ to the data in the above sense. Such oscillations would be regarded as spurious in a representation of an efficiency curve, since they would result in violation of the required smoothness indicated above.

A polynomial might even take negative values in part of the range of interest. A polynomial that took such values at meaningful energies would not provide a physically possible representation of an efficiency curve. In particular, it could not be used for predictive purposes at such energies.

Both oscillations and negative values indeed occurred when using a prototype version of a software implementation based on ‘pure polynomials’.

Two modifications were made to address this aspect. They were based on studying the ‘shape’ of the SIR photon efficiency curve, which is often plotted as $F(\mathbf{B}^{(1)}, E)/E$ against E in order to display more clearly the deviations of the efficiency curve from linearity.

First, a polynomial with argument $\ln E$ rather than E was used in modelling the photon efficiency curve, because the interval of values of E covers three orders of magnitude and the shape of this curve is more polynomial-like when expressed in terms of $\ln E$. The use of this argument helped to overcome problems with spurious oscillations when applied to the measurement data of concern. The principal reason for the improvement is the changes made to the spacing between the relatively sparse radionuclide data available at high energies.

The interval of values of W was such that a logarithmic transformation was not necessary in modelling the electron efficiency curve.

Second, to ensure that a mathematical representation of an efficiency curve could never take a negative value, and therefore remained physically possible, each of the models for $F(\mathbf{B}^{(1)}, E)/E$ and $G(\mathbf{B}^{(2)}, W)/W$ was expressed as the *exponential of a polynomial* rather than a pure polynomial.⁽¹⁾ Such a form is positive everywhere for any polynomial. In fact, this is equivalent to plotting the photon efficiency curve on a log-log scale. The use of the exponential of a polynomial has a further advantage. For the SIR, the graph of $F(\mathbf{B}^{(1)}, E)/E$ constitutes a ‘peak’. In areas such as spectroscopy, peaks are often represented by a Gaussian function or a variant of such a function. A Gaussian function can be written as the exponential of a polynomial of order three.⁽²⁾ For exponentials of polynomials of order greater than three,

⁽¹⁾ A class of models consisting of ‘exponentials of polynomials’ has been used in spectral characteristic modelling [20], behaving like a Gaussian function in a log variable (a ‘log-normal’) for polynomial order three (degree two or quadratic), and providing greater approximation power for higher orders.

various degrees of asymmetry, bulbousness, etc. can be reproduced. This should give the model sufficient flexibility to reproduce the shape of efficiency curves for an ionization chamber different from those of the SIR (see Section 10.2, see p. 46).

The variants of Equation (9) used are thus

$$F(\mathbf{B}^{(1)}, E) = E \exp \left(\sum_{h=1}^n B_h^{(1)} \phi_h(\ln E) \right), \quad (10)$$

$$G(\mathbf{B}^{(2)}, W) = W \exp \left(\sum_{h=1}^{n\beta} B_h^{(2)} \psi_h(W) \right).$$

Now consider how estimates of $\mathbf{B}^{(1)}$ and $\mathbf{B}^{(2)}$ in the Equation (10) can be determined. If these models adequately describe the efficiency curves, that is the approximation errors committed by their use are negligible compared with the uncertainties associated with $\hat{\mathbf{D}}$, $\hat{\mathbf{N}}$ and $\hat{\mathbf{R}}$ (an aspect addressed in Chapter 7, see p. 32), Equation (10) can be substituted into the Equation (8), and the resulting expression employed. Thus,

$$(A_e)_i^{\text{model}}(\mathbf{B}, \mathbf{N}) = \left[\sum_{j \in J_i} P_{i,j} E_{i,j} \exp \left(\sum_{h=1}^n B_h^{(1)} \phi_h(\ln E_{i,j}) \right) + \sum_{j \in \beta J_i} \beta P_{i,j} \int_1^{W_{i,j}} W S_{i,j}(W) \exp \left(\sum_{h=1}^{n\beta} B_h^{(2)} \psi_h(W) \right) dW \right], \quad (11)$$

the form for the model that is used henceforth.

3.2.2. Polynomial representation

For purposes of numerical stability [14], essential here to avoid unnecessary loss of numerical precision for polynomials of arbitrary order, $\phi_h(\ln E)$ in Equation (10) is represented as

$$\phi_h(\ln E) = T_{h-1}(x), \quad (12)$$

where $T_j(x)$ is the Chebyshev polynomial of the first kind of degree j in the normalized variable

$$x = \frac{(\ln E - \ln E_{\min}) - (\ln E_{\max} - \ln E)}{\ln E_{\max} - \ln E_{\min}}, \quad (13)$$

and $[E_{\min}, E_{\max}]$ is the energy range over which the modelling is to be carried out. It is recommended that the values

$$E_{\min} = \min_{j \in I} E_{i,j}, \quad (14)$$

$$E_{\max} = \max_{j \in I} E_{i,j}$$

are taken. Reasons for the specific Equation (13) of the linear transformation formula have been given [11].

The $G(\mathbf{B}^{(2)}, W)$ is treated similarly: $\psi_h(W)$ in Equation (10) is represented as

$$\psi_h(W) = T_{h-1}(x), \quad (15)$$

where

⁽²⁾ The exponential of a polynomial of order three can be expressed in at least two ways, namely, $p_1 \exp(-p_2(E-p_3)^2)$ and $\exp(q_1 + q_2 E + q_3 E^2)$. The first form is a scaled Gaussian function and the second the exponential of a quadratic polynomial. For any value of the Gaussian parameters p_1 , p_2 and p_3 , the polynomial coefficients q_1 , q_2 and q_3 can be formed in terms of them. Conversely, for any polynomial coefficients q_1 , q_2 and q_3 , with $q_3 < 0$, the Gaussian parameters p_1 , p_2 and p_3 can be formed from them. The condition $q_3 < 0$ implies that the function is a 'peak', as opposed to a 'valley'.

$$x = \frac{(W - W_{\min}) - (W_{\max} - W)}{W_{\max} - W_{\min}}, \quad (16)$$

with

$$\begin{aligned} W_{\min} &= 1, \\ W_{\max} &= \max_{j \in I} W_{i,j}. \end{aligned} \quad (17)$$

3.3. Accounting for impurity corrections

Any particular correction $C_{i,f}$ (Section 2.1, see p. 15) is either known or depends on \mathbf{B} , \mathbf{N} and \mathbf{R} , and can thus generally be represented by $C_{i,f}(\mathbf{B}, \mathbf{N}, \mathbf{R})$.

To account for the categories of correction factor considered in Section 2.1, and in order to generalize the treatment, a *mixing ratio* θ_i relating to each radionuclide of concern is introduced. This ratio is taken as unity or zero according to whether or not radionuclide i had previously been well-characterized, that is whether or not a reliable value $(A_e)_i^{\text{KCRV}}$ for the equivalent activity $(A_e)_i$ is available. Then, Equation (5) can be interpreted as

$$C_{i,f}(\mathbf{B}, \mathbf{N}, \mathbf{R}) = 1 + \sum_{k \in K_{i,f}} R_{i,f,k} Q_{i,k}(\mathbf{B}, \mathbf{N}), \quad (18)$$

where

$$Q_{i,k}(\mathbf{B}, \mathbf{N}) = \frac{(A_e)_i^{\text{cmptd}}(\mathbf{B}, \mathbf{N})}{(A_e)_k^{\text{cmptd}}(\mathbf{B}, \mathbf{N})}, \quad (19)$$

and, with the superscript *cmptd* denoting ‘computed’,

$$(A_e)_i^{\text{cmptd}}(\mathbf{B}, \mathbf{N}) = \theta_i (A_e)_i^{\text{KCRV}} + (1 - \theta_i) (A_e)_i^{\text{model}}(\mathbf{B}, \mathbf{N}). \quad (20)$$

This approach has the property that a value of θ_i between zero and one can be chosen to reflect the use of a previously evaluated but not totally reliable value of $(A_e)_i$. The use of θ_i also results in a simplification of the formulae used for derivatives when solving the generalized non-linear least-squares problem and in the uncertainty evaluation (Appendix 2, see p. 56).

4. Solution characterization

4.1. Matching modelled and measured values

Let I denote the set of indices of all radionuclides of concern and L_i the set of indices representing the laboratories that have measured radionuclide i .

The current-, decay- and impurity-corrected quantity (Equation (2), see p. 16) is expressed as

$$(A_e)_{i,\ell}^{\text{meas}}(\mathbf{B}, \mathbf{D}, \mathbf{N}, \mathbf{R}) = D_{i,\ell} C_{i,\ell}(\mathbf{B}, \mathbf{N}, \mathbf{R}). \quad (21)$$

The requirement is to match in some sense the Equation (8) and Equation (21). Both the ‘measured’ and modelled equivalent activities over all relevant radionuclides i and laboratories ℓ generally depend on \mathbf{B} , \mathbf{N} and \mathbf{R} . The latter activities (Equation (21), see p. 24) also depend on \mathbf{D} . Matching is achieved by estimating \mathbf{B} in such a way that a suitable measure of closeness of the two expressions (Section 4.2, see p. 25) is as small as possible. However, the form of the problem is unconventional as a consequence of the ‘measured’ equivalent activities depending on the unknown parameters \mathbf{B} rather than being fixed. The problem can, however, be transformed as follows.

Divide the right-hand sides of Equation (8) and Equation (21) by $C_{i,\ell}(\mathbf{B}, \mathbf{N}, \mathbf{R})$. The advantage of this simple problem transformation is that the $f_{i,\ell}(\mathbf{B}, \mathbf{N}, \mathbf{R})$ given by

$$f_{i,\ell}(\mathbf{B}, \mathbf{N}, \mathbf{R}) = \frac{(A_e)_i^{\text{model}}(\mathbf{B}, \mathbf{N})}{C_{i,\ell}(\mathbf{B}, \mathbf{N}, \mathbf{R})}, \quad i \in I, \ell \in L_i \quad (22)$$

which depend on \mathbf{B} , \mathbf{N} and \mathbf{R} , can then be matched to the $D_{i,\ell}$, which depend only on \mathbf{D} .

The function $f_{i,\ell}(\mathbf{B}, \mathbf{N}, \mathbf{R})$ will be known as the *equivalent activity model* for radionuclide i and laboratory ℓ . The vector of the $f_{i,\ell}(\mathbf{B}, \mathbf{N}, \mathbf{R})$ will be denoted by $f(\mathbf{B}, \mathbf{N}, \mathbf{R})$ and known as the *equivalent activity model vector*.

To reiterate, the information available for use in the determination of a match includes

1. the vector estimate $\hat{\mathbf{D}}$ of \mathbf{D} provided by the laboratories’ measured values of the activities of the radionuclides and by the ionization current measurements in the SIR,
2. a vector estimate $\hat{\mathbf{B}}$ of the efficiency curve parameters \mathbf{B} , e.g. from previous work on determining efficiency curves (see Section 5.4, see p. 29),
3. a vector estimate $\hat{\mathbf{N}}$ of \mathbf{N} from published nuclear reference data,
4. a vector estimate $\hat{\mathbf{R}}$, the elements of which are provided by the laboratories, of the relative impurity activities \mathbf{R} , and
5. the uncertainty matrices associated with the vector estimates in 1)-4).

Denote by \mathbf{Z} the composite vector of quantities \mathbf{B} , \mathbf{N} and \mathbf{R} :

$$\mathbf{Z}^\top = [\mathbf{B}^\top, \mathbf{N}^\top, \mathbf{R}^\top]$$

It is taken that \mathbf{D} and \mathbf{Z} are mutually independent.

4.2. Measure of deviation of model from data

4.2.1. Full formulation

If all the estimates $\hat{\mathbf{D}}$, $\hat{\mathbf{B}}$, $\hat{\mathbf{N}}$ and $\hat{\mathbf{R}}$ and their associated uncertainty matrices, discussed in Section 4.1, are to be used within the generalized non-linear least-squares regression, these estimates can be regarded as *prior* values of the corresponding quantities, and the results of the analysis would furnish *posterior* estimates of these quantities. In this context, denote by $\hat{\mathbf{Z}}$ the corresponding prior estimate of \mathbf{Z} ,

$$\hat{\mathbf{Z}}^\top = [\hat{\mathbf{B}}^\top, \hat{\mathbf{N}}^\top, \hat{\mathbf{R}}^\top],$$

and by $\mathbf{V}_{\hat{\mathbf{Z}}} = \text{diag}(\mathbf{V}_{\hat{\mathbf{B}}}, \mathbf{V}_{\hat{\mathbf{N}}}, \mathbf{V}_{\hat{\mathbf{R}}})$ the uncertainty matrix associated with $\hat{\mathbf{Z}}$.

A measure of the deviation of \mathbf{D} and \mathbf{Z} from their prior estimates that accounts for the provided uncertainty information is

$$(\hat{\mathbf{D}} - \mathbf{D})^\top \mathbf{V}_{\hat{\mathbf{D}}}^{-1} (\hat{\mathbf{D}} - \mathbf{D}) + (\hat{\mathbf{Z}} - \mathbf{Z})^\top \mathbf{V}_{\hat{\mathbf{Z}}}^{-1} (\hat{\mathbf{Z}} - \mathbf{Z}).$$

This formulation constitutes a non-linear counterpart of a Gauss-Markov measure [2].

Since the posterior estimate of \mathbf{D} is to be equal to that of the model vector $f(\mathbf{B}, \mathbf{N}, \mathbf{R}) \equiv f(\mathbf{Z})$, this measure can be expressed as

$$S_{\text{full}}(\mathbf{Z}) = [\hat{\mathbf{D}} - f(\mathbf{Z})]^\top \mathbf{V}_{\hat{\mathbf{D}}}^{-1} [\hat{\mathbf{D}} - f(\mathbf{Z})] + (\hat{\mathbf{Z}} - \mathbf{Z})^\top \mathbf{V}_{\hat{\mathbf{Z}}}^{-1} (\hat{\mathbf{Z}} - \mathbf{Z}). \quad (23)$$

A statistically valid match of model and data would be achieved by minimizing $S_{\text{full}}(\mathbf{Z})$ with respect to \mathbf{Z} to obtain the posterior vector estimate \mathbf{Z}^* , say, of this quantity. The uncertainty matrix $\mathbf{V}_{\mathbf{Z}^*}$ associated with \mathbf{Z}^* could also be obtained as a by-product of the minimization algorithm, from which the required uncertainty matrix $\mathbf{V}_{\mathbf{B}^*}$ associated with \mathbf{B}^* , the posterior estimate of \mathbf{B} , could be extracted.

Were the model linear in the parameters, the corresponding (linear least-squares) estimator would be the most efficient (that is, having minimum variance) of all unbiased estimators that can be expressed in terms of linear functions of the data (from Gauss-Markov theory). For a model that is non-linear in the parameters, as here, that result would apply only approximately. There may exist another estimator that is more efficient, but obtaining such an estimator would be a challenging task.

There are two difficulties associated with the Equation (23), relating to (a) the appreciable amount of computation that would be required to minimize it, and (b) the interpretation and repercussions of the results, leading to several consequences, as indicated in the following paragraph.

The approach formulates *a priori* the problem in a manner that respects the knowledge of the uncertainties associated with all relevant effects. The function $S_{\text{full}}(\mathbf{Z})$ in Equation (23) is minimized with respect to $\mathbf{Z} = [\mathbf{B}^\top, \mathbf{N}^\top, \mathbf{R}^\top]^\top$ to give estimates \mathbf{B}^* of \mathbf{B} , \mathbf{N}^* of \mathbf{N} , and \mathbf{R}^* of \mathbf{R} . If all these estimates were to be ‘accepted’ in some sense, assuming that statistical tests of the model were satisfied, \mathbf{B}^* would provide an improved definition of the efficiency curves. Moreover, \mathbf{N}^* could arguably be used as replacements for the tabulated nuclear reference data. The rationale for this statement is that further information (the SIR measurement data)

has been used, the statistical tests were satisfied (meaning there is no reason to suspect any inconsistency), and hence the adjusted values should constitute improvements. However, it would be unreasonable to expect that the tables of the transition energies and probabilities would be updated on every occasion a statistically consistent model fit was made. Therefore, one approach could be to use the energy curve parameters \mathbf{B}^* so provided, but not explicitly to propose change to the tables of nuclear reference data (although the relevant authors could be informed). Should the model fit be statistically inconsistent with the data, an intriguing possibility is raised. It is recommended in Section 7.1 that following a failure of the consistency check, the model residuals are used to identify radionuclide measurement data regarded as discrepant. This check would naturally also include the nuclear reference data. As a consequence, possible erroneous values for some transition energies and probabilities could be identified.

Similar approaches have been used to determine some nuclear data, such as atomic masses [1].

The full formulation generates a demanding problem computationally. It would appear there is no available software for such problems.⁽¹⁾

⁽¹⁾ It constitutes a generalized non-linear least-squares problem with a number of adjustable parameters equal not just to the dimension of \mathbf{B} (of order 10), but to the dimension of $\mathbf{Z} = [\mathbf{B}^T, \mathbf{N}^T, \mathbf{R}^T]^T$ (of order 1000). Such problems can be solved on today's computers, especially if advantage is taken of the structure of the matrices that arises in their formulation. For the problem of concern here, the Jacobian matrix (Section 1.2, see p. 12) would be bordered (or augmented band) [10] and the uncertainty matrix block-diagonal. Algorithms and software already exist [10], [12] for problems with a bordered Jacobian and a diagonal uncertainty matrix. For the problem here, with a bordered Jacobian and a block-diagonal uncertainty matrix, it seems that software is not available for such a computation, although the technology exists for developing an implementation.

4.2.2. Partial formulation

Instead, therefore, an approach is used that avoids this difficulty, which has good rather than near-optimal statistical properties. The approach does not provide $\mathbf{V}_{\mathbf{Z}^*}$ directly. Rather, this uncertainty matrix is obtained by a stage of uncertainty propagation once \mathbf{B}^* has been determined (Chapter 6, see p. 30).

The Equation (23) is adapted as follows. First, the vector components \mathbf{N} and \mathbf{R} of \mathbf{Z} are not regarded as quantities for which posterior estimates are to be determined. Rather they are set to the prior estimates $\hat{\mathbf{N}}$ and $\hat{\mathbf{R}}$ and kept fixed at these values. Second, no prior estimate of \mathbf{B} is used. (Such an estimate is used, however, as an initial approximation to \mathbf{B} when solving iteratively the problem formulated below.) Consequently, instead of the Equation (23), the measure

$$S_{\text{part}}(\mathbf{B}) = [\hat{\mathbf{D}} - f(\mathbf{B}, \hat{\mathbf{N}}, \hat{\mathbf{R}})]^T \mathbf{V}_{\hat{\mathbf{D}}}^{-1} - f(\mathbf{B}, \hat{\mathbf{N}}, \hat{\mathbf{R}}) \quad (24)$$

is used. This measure, a function of \mathbf{B} only, is minimized with respect to \mathbf{B} using a reliable generalized non-linear least-squares algorithm [2]. The resulting uncertainty matrix associated with the estimate \mathbf{B}^* so determined does not, however, account for the effects of the uncertainty matrices associated with $\hat{\mathbf{N}}$ and $\hat{\mathbf{R}}$. The manner in which such account can be taken is considered in Chapter 6.

In consistent cases this approach based on a partial formulation can be expected to yield only slightly different estimates \mathbf{N}^* from those provided by the full least-squares formulation in Section 4.2.1.

4.3. Equation characterizing the solution

Specifically, \mathbf{B}^* is the \mathbf{B} that minimizes the Equation (24). At the solution, the partial derivatives of the measure with respect to \mathbf{B} are zero. The solution hence satisfies [26]

$$h(\mathbf{B}, \hat{\mathbf{D}}, \hat{\mathbf{N}}, \hat{\mathbf{R}}) \equiv \left(\frac{\partial f(\mathbf{B}, \hat{\mathbf{N}}, \hat{\mathbf{R}})}{\partial \mathbf{B}} \right)^\top \mathbf{V}_{\hat{\mathbf{D}}}^{-1} [\hat{\mathbf{D}} - f(\mathbf{B}, \hat{\mathbf{N}}, \hat{\mathbf{R}})] = 0, \quad (25)$$

where

$$\frac{\partial f(\mathbf{B}, \hat{\mathbf{N}}, \hat{\mathbf{R}})}{\partial \mathbf{B}} = \begin{bmatrix} \partial f_1 / \partial B_1 & \dots & \partial f_1 / \partial B_N \\ \vdots & \ddots & \vdots \\ \partial f_m / \partial B_1 & \dots & \partial f_m / \partial B_N \end{bmatrix}$$

Vector equation Equation (25), constituting a system of non-linear algebraic equations, is not generally solved as such for $\mathbf{B} = \mathbf{B}^*$, but $S_{\text{part}}(\mathbf{B})$ in Equation (24) is minimized using a generalized nonlinear least-squares algorithm to provide \mathbf{B}^* . Equation (25) is, however, important regarding uncertainty evaluation for the solution of the problem (Chapter 6, see p. 30).

5. Model parameter determination

5.1. General

The generalized non-linear least-squares algorithm mentioned in Section 4.2 is iterative. Starting with an initial approximation to \mathbf{B} , at each iteration it constructs what is generally an improved approximation. The sequence of approximations ultimately converge to \mathbf{B}^* . At each iteration, the model deviation

$$s(\mathbf{B}, \mathbf{D}, \mathbf{N}, \mathbf{R}) = \mathbf{D} - f(\mathbf{B}, \mathbf{N}, \mathbf{R}) \quad (26)$$

and the partial derivatives of that deviation with respect to \mathbf{B} are evaluated for the current value of \mathbf{B} , with

$$\mathbf{D} = \hat{\mathbf{D}},$$

$$\mathbf{N} = \hat{\mathbf{N}},$$

$$\mathbf{R} = \hat{\mathbf{R}}.$$

5.2. First-order derivative evaluation

These derivatives constitute the Jacobian matrix

$$\mathbf{J}(\mathbf{B}) = \frac{\partial s(\mathbf{B}, \hat{\mathbf{D}}, \hat{\mathbf{N}}, \hat{\mathbf{R}})}{\partial \mathbf{B}} = -\frac{\partial f(\mathbf{B}, \hat{\mathbf{D}}, \hat{\mathbf{N}}, \hat{\mathbf{R}})}{\partial \mathbf{B}}.$$

The model vector $f(\mathbf{B}, \mathbf{N}, \mathbf{R})$ has components $f_{i,\ell}(\mathbf{B}, \mathbf{N}, \mathbf{R})$ and the model deviation vector $s(\mathbf{B}, \mathbf{D}, \mathbf{N}, \mathbf{R})$ has component deviations $s_{i,\ell}(\mathbf{B}, \mathbf{D}, \mathbf{N}, \mathbf{R})$, with respect to the elements of the efficiency curve parameter vector \mathbf{B} , the decay-corrected measurement vector \mathbf{D} , the nuclear reference data vector \mathbf{N} , and the relative impurity activities vector \mathbf{R} . The components are related by

$$s_{i,\ell}(\mathbf{B}, \mathbf{D}, \mathbf{N}, \mathbf{R}) = D_{i,\ell} - f_{i,\ell}(\mathbf{B}, \mathbf{N}, \mathbf{R}) \quad (27)$$

where, to recapitulate, $D_{i,\ell}$ is an element of \mathbf{D} , and $f_{i,\ell}(\mathbf{B}, \mathbf{N}, \mathbf{R})$ is equal to the quotient of the model function $(A_e)_i^{\text{model}}(\mathbf{B}, \mathbf{N})$ and the parametrized correction term $C_{i,\ell}(\mathbf{B}, \mathbf{N}, \mathbf{R})$. The first set of such derivatives is needed when using an algorithm to solve the generalized non-linear least-squares problem to determine a vector estimate \mathbf{B}^* of \mathbf{B} when the quantities \mathbf{D} , \mathbf{N} and \mathbf{R} are set to their best prior estimates (Section 4.2.2, see p. 26). All these derivatives are needed as part of the evaluation of the uncertainties associated with \mathbf{B}^* .

The various first-order derivatives are given in Appendix 2.

5.3. Use of a generalized non-linear least-squares solver

The solution of the generalized non-linear least-squares formulation of Section 4.2.2 is carried out using a high-quality library software implementation [24] of a recognized algorithm for such problems.

Such an algorithm requires for its operation:

1. A procedure for calculating the residual deviations $s(\mathbf{B}, \mathbf{D}, \mathbf{N}, \mathbf{R})$ given \mathbf{B} , \mathbf{D} , \mathbf{N} and \mathbf{R} . This procedure is based on Equation (27), Equation (22), Equation (12)–Equation (17), Equation (18)–Equation (20);
2. A procedure for calculating the first-order partial derivatives of these deviations with respect to the elements of \mathbf{B} . Appendix 2 gives details.
3. An approximation to the required estimate of \mathbf{B} , to initialize the iterative solution procedure used by the algorithm. Section 5.4 gives details.

Let $(\mathbf{B}^{(1)})^*$ denote the estimate of $\mathbf{B}^{(1)}$, and $(\mathbf{B}^{(2)})^*$ that of $\mathbf{B}^{(2)}$, given by minimizing $S_{\text{part}}(\mathbf{B})$ in Equation (24). Let $\mathbf{B}^* = \left\{ \left[(\mathbf{B}^{(1)})^* \right]^\top, \left[(\mathbf{B}^{(2)})^* \right]^\top \right\}^\top$.

The generalized non-linear least-squares software also provides the uncertainty matrix $\mathbf{V}_{\mathbf{B}^*}$ associated with \mathbf{B}^* . This uncertainty matrix accounts only for $\mathbf{V}_{\mathbf{D}}$, and not $\mathbf{V}_{\mathbf{N}}$ and $\mathbf{V}_{\mathbf{R}}$.

5.4. Initial approximations to the model parameters

The following approach is used to provide initial approximations to the model parameters \mathbf{B} :

1. Provide a set of points (E_s, ε_s) , $s = 1, \dots, q$, adequately covering the energy spectrum of concern. Previously published curves or preliminary results of Monte Carlo simulations or points derived from single photon emitters may be used for this purpose.
2. Solve the (unweighted) linear least-squares problems of fitting the function

$$\sum_{h=1}^n B_h^{(1)} \phi_h(\ln E)$$

to the data $(E_s, \ln(\varepsilon_s/E_s))$, $s = 1, \dots, q$, to obtain approximations to the values of the $B_h^{(1)}$. In carrying out this step, use the approach described in Section 7.1 to provide an appropriate value for n .

3. Carry out the counterpart of Steps 1 and 2 for the electron efficiency curve to obtain approximations to the values of the $B_h^{(2)}$.

6. Model parameter uncertainties

6.1. General

This section is concerned with the evaluation of the uncertainty matrix $\mathbf{V}_{\mathbf{B}^*}$ associated with the vector estimate \mathbf{B}^* of the model parameter vector \mathbf{B} . The evaluation constitutes the propagation of the uncertainties associated with all the data used in the least-squares modelling, namely, the vector $\hat{\mathbf{D}}$ containing the set of the laboratories and SIR decay-corrected measurement data used, the vector $\hat{\mathbf{N}}$ of relevant published values of the nuclear reference data \mathbf{N} used, and the estimate $\hat{\mathbf{R}}$ of the relative impurity activities vector \mathbf{R} used. For this purpose, the vector estimates $\hat{\mathbf{D}}$, $\hat{\mathbf{N}}$ and $\hat{\mathbf{R}}$ are available, as are the associated uncertainty matrices $\mathbf{V}_{\hat{\mathbf{D}}}$, $\mathbf{V}_{\hat{\mathbf{N}}}$ and $\mathbf{V}_{\hat{\mathbf{R}}}$.⁽¹⁾

⁽¹⁾ The elements of \mathbf{D} may not be independent of those of \mathbf{N} , but information on the correlations is not readily available, other than that the effects would be expected to be small. Therefore, consideration is not given to this form of correlation, although an extension of the analysis here is possible should they be quantifiable.

6.2. Implicit model

The contribution to $\mathbf{V}_{\mathbf{B}^*}$ from $\mathbf{V}_{\hat{\mathbf{D}}}$ is already provided as part of the least-squares solution process (Section 5.3, see p. 28). That contribution is identical to that obtained by uncertainty propagation as considered here applied to $\mathbf{V}_{\hat{\mathbf{D}}}$ alone.

Since \mathbf{B} is related to \mathbf{D} , \mathbf{N} and \mathbf{R} through a least-squares minimization process, rather than there being an *explicit* expression for \mathbf{B} in terms of these quantities, \mathbf{B} satisfies an *implicit* vector function

$$h(\mathbf{B}, \mathbf{D}, \mathbf{N}, \mathbf{R}) = 0, \quad (28)$$

given by differentiating with respect to \mathbf{B} the function to be minimized and equating the result to 0.

The solution \mathbf{B}^* is the \mathbf{B} satisfying Equation (28) after setting \mathbf{D} , \mathbf{N} and \mathbf{R} to their best prior estimates.

The form of the vector function h is identical to that in Equation (25) except that the quantities \mathbf{D} , \mathbf{N} and \mathbf{R} rather than the estimates $\hat{\mathbf{D}}$, $\hat{\mathbf{N}}$ and $\hat{\mathbf{R}}$ are involved, but the uncertainty matrix $\mathbf{V}_{\hat{\mathbf{D}}}$ associated with $\hat{\mathbf{D}}$ is retained:

$$h(\mathbf{B}, \mathbf{D}, \mathbf{N}, \mathbf{R}) \equiv \left(\frac{\partial f(\mathbf{B}, \mathbf{N}, \mathbf{R})}{\partial \mathbf{B}} \right)^T \mathbf{V}_{\hat{\mathbf{D}}}^{-1} [\mathbf{D} - f(\mathbf{B}, \mathbf{N}, \mathbf{R})] = 0.$$

The least-squares solution \mathbf{B}^* satisfies Equation (25) *per se*, and $\mathbf{V}_{\mathbf{B}^*}$ satisfies the matrix equation⁽¹⁾

$$\left[\mathbf{H}_{\mathbf{B}} \mathbf{V}_{\mathbf{B}^*} \mathbf{H}_{\mathbf{B}}^T - \sum_{\alpha=\mathbf{D}, \mathbf{N}, \mathbf{R}} \mathbf{H}_{\alpha} \mathbf{V}_{\hat{\alpha}} \mathbf{H}_{\alpha}^T \right]_{\mathbf{B}=\mathbf{B}^*, \mathbf{D}=\hat{\mathbf{D}}, \mathbf{N}=\hat{\mathbf{N}}, \mathbf{R}=\hat{\mathbf{R}}} = 0, \quad (29)$$

where the *Hessian matrices* $\mathbf{H}_{\mathbf{B}}$ and \mathbf{H}_{α}

$$\mathbf{H}_{\mathbf{B}} = \frac{\partial h}{\partial \mathbf{B}},$$

⁽¹⁾ Equation (29) is obtained by applying the treatment of real implicit multivariate models in a best-practice guide on uncertainty evaluation [17]. In the notation of that guide, the model is

$$h(\mathbf{Y}, \mathbf{X}) = 0,$$

where \mathbf{X} is a vector input quantity and \mathbf{Y} a vector output quantity. Given an estimate $\hat{\mathbf{X}}$ of \mathbf{X} , the

$$\mathbf{H}_\alpha = \frac{\partial h}{\partial \alpha}.$$

Expressions for $\mathbf{H}_\mathbf{B}$ and the \mathbf{H}_α are given in Appendix 3.

estimate $\hat{\mathbf{Y}}$ of \mathbf{Y} is given by solving

$$h(\hat{\mathbf{Y}}, \hat{\mathbf{X}}) = 0.$$

In terms of the Jacobian matrices (Jacobians with respect to h , but Hessians with respect to f),

$$\mathbf{J}(\hat{\mathbf{X}}) = \frac{\partial h}{\partial \mathbf{X}},$$

$$\mathbf{J}(\hat{\mathbf{Y}}) = \frac{\partial h}{\partial \mathbf{Y}},$$

the uncertainty matrix $\mathbf{V}_{\hat{\mathbf{Y}}}$ associated with $\hat{\mathbf{Y}}$ is related to that, $\mathbf{V}_{\hat{\mathbf{X}}}$, associated with $\hat{\mathbf{X}}$, by

$$\mathbf{J}(\hat{\mathbf{Y}})\mathbf{V}_{\hat{\mathbf{Y}}}\mathbf{J}^T(\hat{\mathbf{Y}}) = \mathbf{J}(\hat{\mathbf{X}})\mathbf{V}_{\hat{\mathbf{X}}}\mathbf{J}^T(\hat{\mathbf{X}}),$$

a system of linear equations that is solved for $\mathbf{V}_{\hat{\mathbf{Y}}}$. The extension of this result when \mathbf{X} corresponds to the set of mutually independent vector quantities \mathbf{D} , \mathbf{N} and \mathbf{R} , and \mathbf{Y} to \mathbf{B} , constitutes Equation (29). A numerical procedure for solving Equation (29) for $\mathbf{V}_{\mathbf{B}^*}$ is given in Appendix 4.

7. Validation of model and uncertainty evaluation

Unless the model itself and aspects relating to the model are validated, the results produced may not be reliable. Therefore, attention is paid to the following issues:

1. The choice of models from families of (e.g. polynomial or spline) models;
2. Consistency of model and data;
3. Uncertainty evaluation;
4. Adequacy of quadrature rules (needed in forming the integrals in Equation (11), see p. 22).

7.1. Choice of models from model families

The problem as posed requires choices for the values of n and n_β , the orders (numbers of coefficients) in the Equation (10). It is necessary to deduce suitable orders to generate a model that is consistent with the data.

For problems in fields where there is just one model curve (strictly a family of models) containing a number of coefficients to be determined, a common approach [13] is to fit the model a number of times, with increasing order of model, namely with 1, 2, ... coefficients. For each model order, the *chi-squared ratio*, defined as the ratio of the observed chi-squared value and a critical value of the chi-squared distribution is formed. The observed chi-squared value is the value $S_{\text{full}}(\mathbf{Z})$ in Equation (23) evaluated at the solution $\mathbf{Z}^* = \left((\mathbf{B}^*)^\top, (\hat{\mathbf{N}})^\top, (\hat{\mathbf{R}})^\top \right)^\top$.⁽¹⁾

The chi-squared distribution used is that for a degrees of freedom equal to the number of data less the number of model parameters. The critical point of the chi-squared distribution is that corresponding to an appropriate percentile of that distribution. If the family of models is appropriate for the data and the associated uncertainties, it can be expected that, for a sufficiently high order, the chi-squared ratio will saturate to a value approximately equal to unity. The model of lowest order corresponding to this saturation level can be taken as the required model.

For the models in Equation (11), a different strategy is required, because a choice of two model orders is to be made. The following approach is used. Select provisional values n^{max} and n_β^{max} for the largest plausible values of n and n_β to be considered, for example, based on previous work on obtaining efficiency curves. There are $n^{\text{max}} \times n_\beta^{\text{max}}$ pairs of values in all. For each possible pair from the $n^{\text{max}} \times n_\beta^{\text{max}}$ pairs, fit the corresponding model and form the chi-squared ratio. Arrange these values into a rectangular array of dimensions $n^{\text{max}} \times n_\beta^{\text{max}}$. If the chi-squared ratio saturates to unity within the body of the array, the provisional maximum orders can be regarded as sufficient. Otherwise, choose one or two larger orders, as appropriate, and carry out the necessary additional computations to complete the larger array.

Once an array containing saturation has been obtained, select appropriate orders. The strategy for this selection evolves as experience is gained with the use of the models. Since the electron efficiency curve is simpler in form, a polynomial of low order, such as three, would be expected to suffice in this case. A polynomial of higher order would be required in the

⁽¹⁾ It is essential to use $S_{\text{full}}(\mathbf{Z})$ rather than $S_{\text{part}}(\mathbf{B})$ in Equation (24). The latter only takes uncertainties associated with $\hat{\mathbf{D}}$ into account, whereas the former also accounts for those associated with $\hat{\mathbf{N}}$ and $\hat{\mathbf{R}}$.

modelling of the photon efficiency curve. This information helps to inform the decision regarding choices of model order.

In practice, this statistical approach to model selection was not implemented in the software presented in Chapter 9, since it was straightforward to handle this aspect manually.

7.2. Consistency of model and data

This section provides a test, under the assumption of normality of the various quantities involved, for the consistency of the model and the data.

Form the value of the Equation (23) at the solution $\mathbf{B} = \mathbf{B}^*$. This value is a computed value of chi-squared for $\nu = m - n - n_\beta$ degrees of freedom, the number of measured data (the dimension of \mathbf{D}) less the number of model parameters. If the probability of the value of the chi-squared distribution for ν degrees of freedom exceeding this computed chi-squared value is less than 0.0001, the consistency check is regarded as failed. The use of this probability corresponds to four standard deviations under a normality assumption. This check is actually less stringent than that often recommended in the context of key comparison data evaluation [15], [34].

7.3. Determining a consistent subset

A normalized deviation is defined as a model deviation in Equation (26) normalized by the standard uncertainty associated with this deviation. The corresponding component of $\hat{\mathbf{D}}$ is classified as discrepant if the magnitude of this normalized deviation exceeds 4. This threshold has been adopted by the Section II of the Consultative Committee for Ionizing Radiation [33].

Approaches have been used in key comparison data evaluation [21], [34] for determining a consistent subset based on a successive exclusion strategy. Such a strategy involves excluding one by one those measurement results judged to be discrepant until a consistent subset is obtained. For the present problem, a variant of that procedure is used:

1. Set the current subset \mathbf{I}_D to the set of indices relating to the vector \mathbf{D} of equivalent activity measurement quantities for the radionuclides and laboratories of concern;
2. Fit the model to the data identified by \mathbf{I}_D ;
3. Carry out the consistency test described in Section 7.1 for this data;
4. Finish if the test is satisfied, accepting \mathbf{I}_D as identifying a subset of consistent data and the corresponding \mathbf{B}^* as estimates of the parameters of the efficiency curves;
5. Identify the most discrepant components of $\hat{\mathbf{D}}$ in the subset, namely those for which the magnitude of the normalized deviation exceeds four;
6. Exclude these measurement components from further consideration: remove the index of these results from \mathbf{I}_D ;
7. Return to 2).

Normally, this procedure is cycled once or twice. In the software implementation SIRIC (Chapter 9, see p. 38), the user has the option to perform just one cycle, in which case a

computed chi-squared value for the whole data set is provided, together with a list of discrepant components of $\hat{\mathbf{D}}$. This option corresponds to steps 1)–5) (executed once).

7.4. Uncertainty check by Monte Carlo calculation

Arguably the simplest form of validation of the uncertainties provided by direct evaluation is the use of the propagation of distributions, implemented using a Monte Carlo method (MCM). To apply MCM, first a joint probability density function (PDF) is assigned to the input quantity \mathbf{N} . Invoking the maximum entropy principle implies that a Gaussian PDF should be so assigned. This Gaussian PDF has vector expectation $\hat{\mathbf{N}}$ and covariance matrix $\mathbf{V}_{\hat{\mathbf{N}}}$. Also, on a similar basis, assign PDFs to the vector quantities \mathbf{R} of relative radioactive impurities and \mathbf{D} of the decay-corrected measurement quantities.

The Monte Carlo calculation consists of a large number N_{MC} of trials. Each trial comprises the determination of a realization of the vector quantity \mathbf{B} given a realization of the vector values of \mathbf{N} , \mathbf{R} and \mathbf{D} . Each realization of the vector quantities \mathbf{N} , \mathbf{R} and \mathbf{D} is given by sampling randomly from the above joint PDFs. The N_{MC} realizations of the vector value of \mathbf{B} are assembled into an $(n + n_{\beta}) \times N_{\text{MC}}$ matrix. Let \mathbf{B}_{MC} denote this matrix after correcting each row by its arithmetic mean. Then, $\mathbf{B}_{\text{MC}}(\mathbf{B}_{\text{MC}})^{\top}$ provides an approximation to $\mathbf{V}_{\hat{\mathbf{B}}}$, which is compared with $\mathbf{V}_{\hat{\mathbf{B}}}$ as provided.

If the comparison is favourable, it may reasonably be concluded that the software implementation is sound. There may be two reasons for an unfavourable comparison. One, the software implementation is inadequate. Two, the extent of the non-linearity of the model is such that the above approximation to $\mathbf{V}_{\hat{\mathbf{B}}}$ is better than $\mathbf{V}_{\hat{\mathbf{B}}}$ itself because of the non-linearity of the model. (The law of propagation of uncertainty is based on a linear approximation.) See Chapter 11.

7.5. Adequacy of quadrature rule

Consider the use of a quadrature rule for carrying out the integrations required when evaluating $(A_e)_i^{\text{model}}(\mathbf{B}, \mathbf{N})$ for any particular values of \mathbf{B} in Equation (11). The results of the overall computation can subsequently be confirmed, or re-determined, as appropriate, using a rule with a larger number of quadrature rule nodes. The extent of the agreement that should be sought would be a numerical precision that is at least an order of magnitude smaller than the uncertainties associated with the corresponding results.

The manner in which the integrals in Equation (11) are evaluated numerically would ideally take into account the nature of the integrands and how the energy distribution functions $S_{i,j}(W)$ are specified. However, to avoid the potential difficulties⁽¹⁾ associated with the choice of an adaptive quadrature rule, a fixed-point rule, e.g. the trapezoidal rule, with a large number of nodes, could be used.

⁽¹⁾ Difficulties arise because an adaptive quadrature rule induces discontinuities in the function that can adversely affect the behaviour of the optimization algorithm used to determine the model parameters. Each evaluation of the function would be influenced by the numerical precision, δ_q , say, prescribed for the quadrature scheme. Each function value will

be accurate to within a quantity depending on δ_q , and thus not be smooth, with a deleterious effect on convergence (the convergence proofs for the method would no longer apply), and even introduce spurious local minima in the neighbourhood of the required global solution.

8. Determination of the required quantities and the associated uncertainty evaluation

The primary quantities of interest are

- parameters of the photon and electron efficiency curves,
- corrected measured equivalent activities, and
- modelled equivalent activities.

This section provides the method used to obtain the estimates and associated standard uncertainties of these quantities. All this information can be obtained once parameter vector \mathbf{B} of the efficiency curves has been estimated and the associated uncertainty matrix evaluated.

8.1. Parameters of the photon and electron efficiency curves

The solution provided by the generalized non-linear least-squares algorithm constitutes an estimate \mathbf{B}^* of the efficiency curve parameter vector \mathbf{B} . This estimate can be used to obtain estimates of quantities that depend on \mathbf{B} such as the modelled equivalent activities (Section 8.3, see p. 37).

The generalized non-linear least-squares algorithm provides the contribution from the uncertainty matrix \mathbf{V}_D associated with $\hat{\mathbf{D}}$, to the uncertainty matrix \mathbf{V}_{B^*} associated with \mathbf{B}^* .

Chapter 6 describes the manner in which the contributions from the uncertainty matrices $\mathbf{V}_{\hat{\mathbf{N}}}$ and $\mathbf{V}_{\hat{\mathbf{R}}}$ associated with $\hat{\mathbf{N}}$ and $\hat{\mathbf{R}}$ can also be taken into account following the determination of the least-squares solution.

8.2. Corrected measured equivalent activity

Equation (21) is used for each radionuclide considered and each laboratory concerned to provide corrected measured equivalent activities based on the laboratory and SIR measured values and the modelled correction factor. The estimate provided by Equation (21) based on measurement and modelled correction factors for radionuclide i and laboratory ℓ is

$$\left(\hat{A}_e\right)_{i,\ell}^{\text{meas}} = \hat{D}_{i,\ell} C_{i,\ell} \left(\mathbf{B}^*, \hat{\mathbf{N}}, \hat{\mathbf{R}}\right). \quad (30)$$

The application of the law of propagation of uncertainty to Equation (21) yields the standard uncertainty $u\left(\left(\hat{A}_e\right)_{i,\ell}^{\text{meas}}\right)$ given by

$$u^2\left(\left(\hat{A}_e\right)_{i,\ell}^{\text{meas}}\right) = C_{i,\ell}^2\left(\mathbf{B}^*, \hat{\mathbf{N}}, \hat{\mathbf{R}}\right) u^2\left(\hat{D}_{i,\ell}\right) + \hat{D}_{i,\ell}^2 \left[\left(\frac{\partial C_{i,\ell}(\mathbf{B}, \mathbf{N}, \mathbf{R})}{\partial \mathbf{Z}} \right)^T \mathbf{V}_{\mathbf{Z}^*} \frac{\partial C_{i,\ell}(\mathbf{B}, \mathbf{N}, \mathbf{R})}{\partial \mathbf{Z}} \right]_{\mathbf{Z}=\mathbf{Z}^*} \quad (31)$$

where here

$$\mathbf{Z} = (\mathbf{B}^T, \mathbf{N}^T, \mathbf{R}^T)^T,$$

$$\mathbf{Z}^* = \left((\mathbf{B}^*)^T, \hat{\mathbf{N}}^T, \hat{\mathbf{R}}^T \right)^T.$$

The partial derivatives required in Equation (31) are given in Appendix A2.2.1.

8.3. Modelled equivalent activity

Estimates of modelled equivalent activities are provided by Equation (8). For radionuclide i ,

$$\left(\hat{A}_e\right)_i^{\text{model}} = (A_e)_i^{\text{model}}(\mathbf{B}^*, \hat{\mathbf{N}}). \quad (32)$$

The application of the law of propagation of uncertainty to Equation (8) yields the standard uncertainty $u\left(\left(\hat{A}_e\right)_i^{\text{model}}\right)$ given by

$$u\left(\left(\hat{A}_e\right)_i^{\text{model}}\right) = \left[\left(\frac{\partial (A_e)_i^{\text{model}}(\mathbf{B}, \mathbf{N})}{\partial \mathbf{Z}} \right)^{\top} \mathbf{V}_{\mathbf{Z}^*} \left(\frac{\partial (A_e)_i^{\text{model}}(\mathbf{B}, \mathbf{N})}{\partial \mathbf{Z}} \right) \right]_{\mathbf{Z}=\mathbf{Z}^*} \quad (33)$$

where here

$$\mathbf{Z} = (\mathbf{B}^{\top}, \mathbf{N}^{\top})^{\top},$$

$$\mathbf{Z}^* = \left((\mathbf{B}^*)^{\top}, \hat{\mathbf{N}}^{\top} \right)^{\top}.$$

The partial derivatives required in Equation (33) are given in Appendix A2.2.2 and Appendix A2.2.3.

9. Summary of computational procedure

This section describes the computational procedure, relating its elements to the various sections and formulations in this work. This procedure has been implemented as software known as SIRIC [32], using the Fortran 95 language and the NAG Library(<http://www.nag.co.uk/>). There are some differences between this implementation and the described approach, as indicated in Chapter 11.

Overall, the procedure constitutes the steps:

1. Data input;
2. Efficiency curve generation;
3. Uncertainty evaluation for the efficiency curve parameters;
4. Model-data consistency testing and data exclusion;
5. Efficiency curve interpolation and associated uncertainty evaluation;
6. Results output.

The first five of these steps are subdivided into action points as follows.

Data input

1. Read the control data corresponding to items such as the names of the data files holding the activity measurement data and the nuclear reference data, and also the maximum orders of polynomial to be used in the model.
2. Read nuclear reference data constituting $\{E_{i,j} : j \in J_i\}$, $\{P_{i,j} : j \in J_i\}$, $\{W_{i,j} : j \in \beta J_i\}$ and $\{\beta P_{i,j} : j \in \beta J_i\}$, for all relevant radionuclides i , the associated standard uncertainties, and other relevant items (Section 2.1, see p. 15).
3. Read measurement data constituting the decay-corrected measurement data $D_{i,\ell}$ corresponding to the activity measurement data $A_{i,\ell}$ provided by the laboratories multiplied by the SIR measurement value $M_{i,\ell}$, and the associated standard uncertainties $u(D_{i,\ell})$ (Section 2.1, see p. 15). Also read the impurity activities and their associated standard uncertainties and the relevant radionuclide and impurity names.
4. Read key comparison reference data, namely, the KCRVs for the radionuclides of concern and their associated uncertainties (Section 2.4, see p. 18). Also read the mixing ratios θ_i (Section 3.3, see p. 23), usually equal to zero or one.
5. Read initial efficiency values (E_s, ε_s) needed to start the non-linear least-squares minimization. See Section 5.4.
6. Perform other operations including the determination of atomic number and mass for the relevant radionuclides, which are needed for the evaluation of the shapes of the beta spectra $S_{i,j}$.

Efficiency curve generation

1. Transform the data, namely (a) transform the gamma energies to logarithmic units, (b) transform the electron energies to natural units, and © normalize both transformed energies to forms suitable for polynomial approximation based on a Chebyshev representation (Section 3.2.2, see p. 22).

2. Link the nuclear reference data to the decay-corrected measurement data, and the nuclear reference data and the KCRV data to the impurity data for each measurement.
3. Provide initial approximations to the efficiency curve parameters by applying the method of Section 5.4.
4. Solve a generalized non-linear least-squares problem to provide estimates of the efficiency curve parameters (Section 5.3, see p. 28), using the initial approximations as a starting point.

Uncertainty evaluation for the efficiency curve parameters

1. Evaluate, at the solution of the generalized non-linear least-squares problem, the Jacobian matrices associated with the model equations for each of the input quantities having an associated uncertainty (Appendix 2, see p. 56).
2. Propagate the uncertainty matrices associated with the relative activity impurities and the nuclear reference data, using the evaluated Jacobian matrices, through the generalized non-linear least-squares model to provide the uncertainty matrix associated with the efficiency curve parameters (Chapter 6, see p. 30). This propagation, together with the action above, constitutes an implementation of the partial formulation (Section 4.2.2, see p. 26).

Model-data consistency and determination of a consistent data subset

1. Test for consistency of the fitted model and the data (Section 7.1, see p. 32).
2. Determine a consistent subset of the data by employing a data exclusion strategy (Section 7.3, see p. 33).

Efficiency curve interpolation and associated uncertainty evaluation

1. Produce the efficiency curves defined by the parameter estimates \mathbf{B}^* (Section 3.2.1, see p. 20).
2. Determine the modelled equivalent activity corresponding to each radionuclide and evaluate the associated standard uncertainty (Section 8.3, see p. 37).
3. Determine the measured equivalent activity corrected for impurities corresponding to each data value and evaluate the associated standard uncertainty (Section 8.2, see p. 36).

10. Results

10.1. Application of the procedure to the SIR

The SIRIC software, which applies the procedure described in this monograph, was used to produce the efficiency curves of the SIR. About 275 input A_e^{meas} values covering 40 different radionuclides, including four pure beta emitters, were used. Radionuclides for which fewer than two SIR results based on primary standardizations are available were excluded from the minimization, but were used to test the predictive capabilities of SIRIC. The radionuclides ^{65}Zn , ^{67}Ga , ^{99}Mo , ^{153}Gd , ^{169}Yb , ^{177}Lu and ^{201}Tl were excluded because either the SIR values or the nuclear data were not considered sufficiently robust. On the other hand, the ^{125}I SIR results are essential to constrain the photon efficiency curve at low energy, even though these results were not considered sufficiently reliable to establish the ^{125}I KCRV. Similarly, the ^{124}Sb SIR data are used in the minimization to constrain better the high energy part of the photon curve, despite these data exhibiting discrepancies that are perhaps related to the different standardization methods. As the ionization chamber response is not expected to be the same for gases and β^+ emitters, those radionuclides were also excluded, except ^{56}Co that is needed to constrain the photon efficiency curve at high energy.

The nuclear data used were taken from the first two volumes of Monographie BIPM-5 [4], the Decay Data Evaluation Project 2004 database [25] and, when not otherwise available, from the 2004 Evaluated Nuclear Structure Data File [35]. In order to speed up the execution of the software, a 20keV cut-off for photon energy, a 10^{-5} cut-off for photon intensities and 10^{-3} cut-off for beta emission probabilities were applied. Indeed, these choices of cut-off values enable a saving of time that would otherwise be spent in handling radiations that would anyway have a negligible effect on the results.

The chosen cut-off values should be optimized for each type of ionization chamber. In the case of the SIR, the cut-off should not be higher than 20keV in order to include the ^{109}Cd x-rays. A run of SIRIC with one preliminary cycle to exclude discrepant data (see Section 7.3, see p. 33) takes about two hours with a Pentium 4 (2GHz) processor, most of this time being dedicated to the uncertainty calculation related to the nuclear data due to the volume of data involved.

As indicated in Section 5.4, initial efficiency values are needed to start the least-squares minimization. The values used for the photon efficiency curve of the SIR are given in Table 1 and are based on quasi-monoenergetic photon emitters. Indeed, for such radionuclides, the efficiency value ε_s at energy E_s can easily be calculated from $\varepsilon_s = 1/((A_e)_i^{\text{meas}} P_s)$, with $E_s = E_{i,j}$ and $P_s = P_{i,j}$. For a radionuclide such as ^{60}Co , emitting only two photons with close energies E_1 and E_2 and intensities P_1 and P_2 ,

$$E_s = \frac{E_1 P_1 + E_2 P_2}{P_1 + P_2}$$

and

$$P_s = P_1 + P_2.$$

Table 1. Initial values used for the photon efficiency curve.

Radionuclide	E_s/keV	ε_s
--------------	------------------	-----------------

—	30.0	1.00×10^{-8}
^{241}Am	59.5	1.35×10^{-6}
^{109}Cd	88.0	3.39×10^{-6}
^{57}Co	123.7	6.16×10^{-6}
$^{99}\text{Tc}^{\text{m}}$	140.5	7.34×10^{-6}
^{47}Sc	159.4	8.95×10^{-6}
^{111}In	209.0	1.26×10^{-5}
^{51}Cr	320.1	2.08×10^{-5}
^{85}Sr	514.0	3.40×10^{-5}
^{137}Cs	661.7	4.27×10^{-5}
^{95}Nb	765.8	4.84×10^{-5}
^{54}Mn	834.8	5.20×10^{-5}
^{46}Sc	1 004.9	6.01×10^{-5}
^{60}Co	1 252.9	7.09×10^{-5}
^{88}Y	1 380.0	7.50×10^{-5}
^{24}Na	2 061.3	1.01×10^{-4}

For the electron efficiency curve, the initial values were taken from the curve obtained by the iterative method [31]. Although in the iterative method, beta spectra were replaced by delta functions at the mean beta energy, the resulting efficiency values were found satisfactory as initial values for SIRIC.

The choice of orders for the ‘photon polynomial’ and the ‘electron polynomial’ in the model was based on the chi-squared ratio

$$\frac{\chi_{\text{obs}}^2}{\chi_{\text{crit}}^2},$$

where χ_{obs}^2 is the observed chi-squared value and χ_{crit}^2 is the critical value of the chi-squared distribution for the appropriate degrees of freedom ν (Section 7.1, see p. 32). Relevant results for appropriate polynomial orders that led to the orders selected are shown in Table 2. The different values for the degrees of freedom ν are due to different numbers of measurement results excluded at the end of the first cycle of SIRIC (Section 7.3, see p. 33).

Table 2. Chi-squared values, chi-squared ratios and degrees of freedom for relevant orders n and n_{β} , respectively, of the ‘photon polynomial’ and the ‘electron polynomial’ in the model.

Polynomial orders		$n_{\beta} = 4$	$n_{\beta} = 5$	$n_{\beta} = 6$
$n = 8$	χ_{obs}^2	400	399	383
	ν	234	234	233
	χ_{crit}^2	323	323	322
	χ^2 ratio	1.24	1.24	1.19
$n = 9$	χ_{obs}^2	366	367	350
	ν	234	234	230
	χ_{crit}^2	323	323	318
	χ^2 ratio	1.13	1.14	1.10
$n = 10$	χ_{obs}^2	366	367	350
	ν	233	233	229
	χ_{crit}^2	322	322	317

χ^2 ratio	1.14	1.14	1.10
----------------	------	------	------

The cases $n_\beta=6$ with $n=9$ and 10 were excluded from further consideration because the corresponding electron efficiency curves diverge at high energy. Since order 10 for the photon polynomial does not improve the chi-squared ratio, $n=9$ is selected. For the electron polynomial, $n_\beta=5$ is preferred to $n_\beta=4$ since the corresponding fifth-order electron efficiency curve displays a behaviour closer to preliminary Monte Carlo simulation results [32].

The values of the parameter vector \mathbf{B}^* obtained with $n=9$ and $n_\beta=5$ are listed in Table 3. The uncertainty values given are the square root of the diagonal elements of the uncertainty matrix V_B^* . The corresponding photon efficiency curve $F\left(\left(\mathbf{B}^{(1)}\right)^*, E\right)$ and electron efficiency curve $G\left(\left(\mathbf{B}^{(2)}\right)^*, W\right)$ (cf. Section 3.2.1, see p. 20) are shown in Figure 1 and Figure 3. The energy ranges covered are [20keV, 3866.14keV] and [1, 7.93] for the photon energy E and the reduced total electron energy W respectively.

Table 3. Values and uncertainties of the efficiency curve parameters $\left(B_h^{(1)}\right)^*$ and $\left(B_h^{(2)}\right)^*$ obtained with $n=9$ and $n_\beta=5$.

h	Photon efficiency curve		Electron efficiency curve	
	$\left(B_h^{(1)}\right)^*$	$u\left(\left(B_h^{(1)}\right)^*\right)$	$\left(B_h^{(2)}\right)^*$	$u\left(\left(B_h^{(2)}\right)^*\right)$
1	-37.84	0.05	-30.2	0.3
2	3.91	0.04	4.76	0.18
3	-3.33	0.05	-0.6	0.2
4	2.07	0.04	0.61	0.10
5	-1.28	0.04	-0.62	0.09
6	0.71	0.02		
7	-0.35	0.02		
8	0.128	0.009		
9	-0.049	0.006		

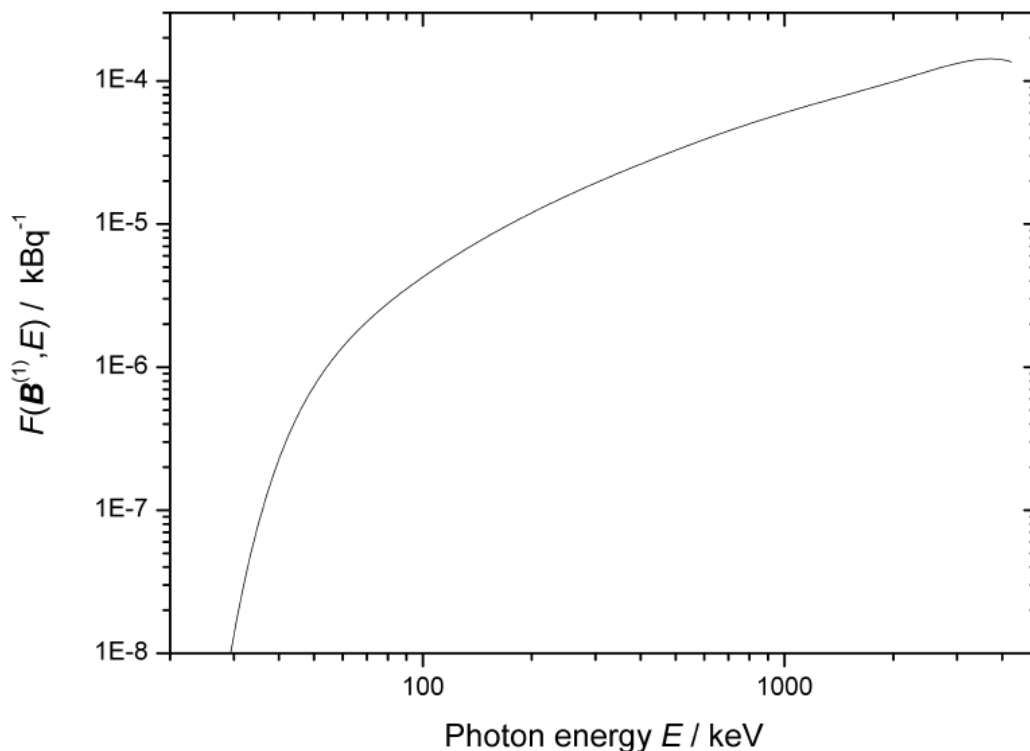


Figure 1 — SIR photon efficiency curve.

It should be noted that these results were obtained after data exclusion carried out automatically by SIRIC following procedure Section 7.3. At the end of the first cycle, the observed chi-squared value was 502 with $\nu = 240$ and SIRIC identified 6 SIR results to be excluded (one result for each of the following radionuclides: ^{111}In , ^{124}Sb , ^{134}Cs , ^{137}Cs , ^{106}Ru , ^{204}Tl).

The photon efficiency function obtained, scaled by $6 \times 10^{-8}E$, that is $F(\mathbf{B}^{(1)*}, E)/6 \times 10^{-8}E$, is shown in Figure 2 (upper) (cf. Section 3.2.1, see p. 20). The relative standard uncertainty associated with the curve is shown with the ordinate on the right-hand side.

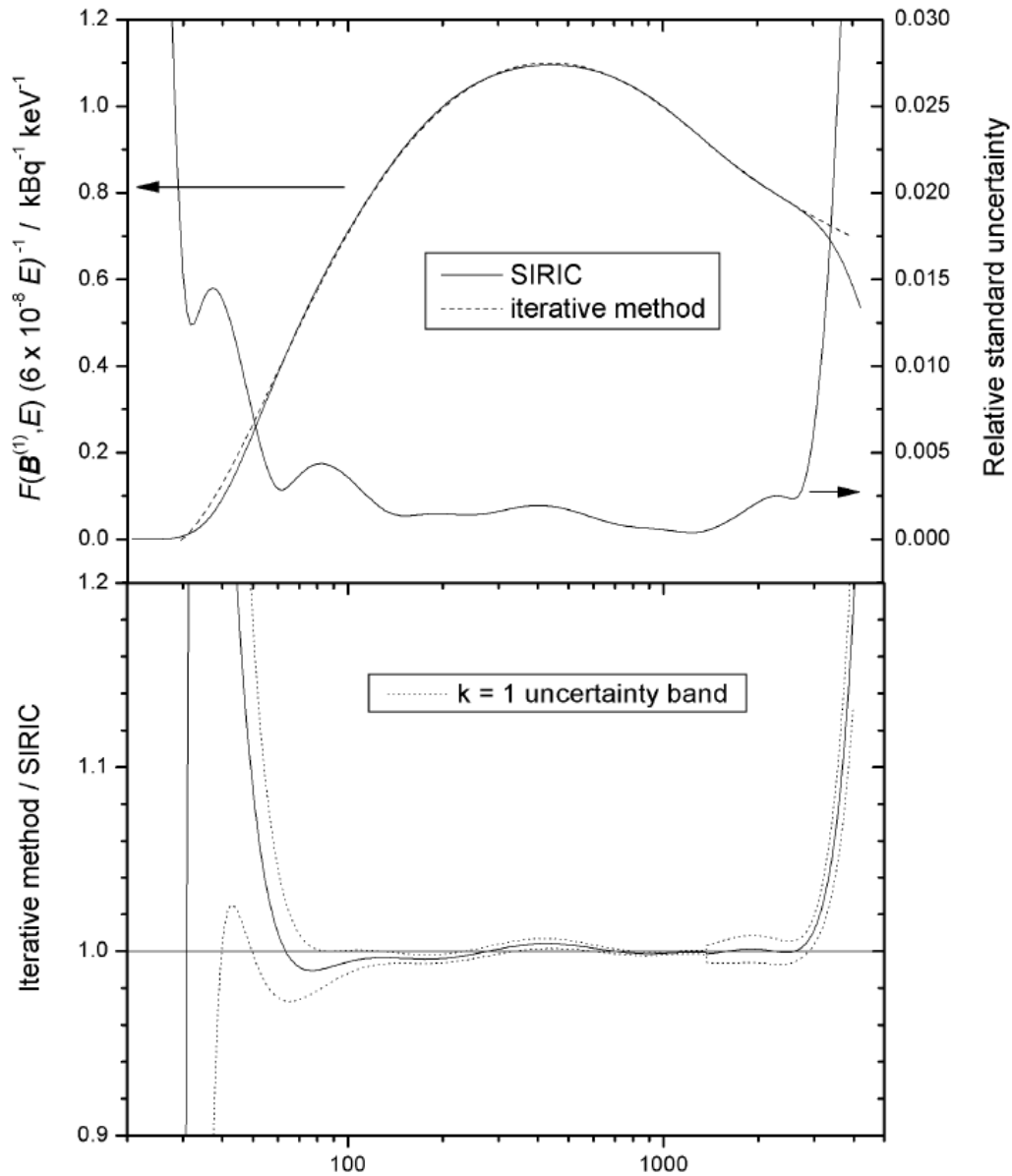


Figure 2 — SIR photon efficiency curve: comparison of the curve obtained applying the present procedure (SIRIC software) with the curve published in 2002 based on the iterative method [31].

Figure 2 (upper) also shows, for comparison, the curve obtained by the iterative method (Chapter 1, see p. 10) [31]. Figure 2 (lower) shows the ratio of both curves and their combined standard uncertainty. Both curves agree within one standard uncertainty except at high energy, where the SIRIC curve seems to display inappropriate behaviour due to the lack of data to constrain the minimization at high energy. It should be noted that the SIRIC curve behaves satisfactorily at low energy, as opposed to the 2002 curve that was negative below 30keV.

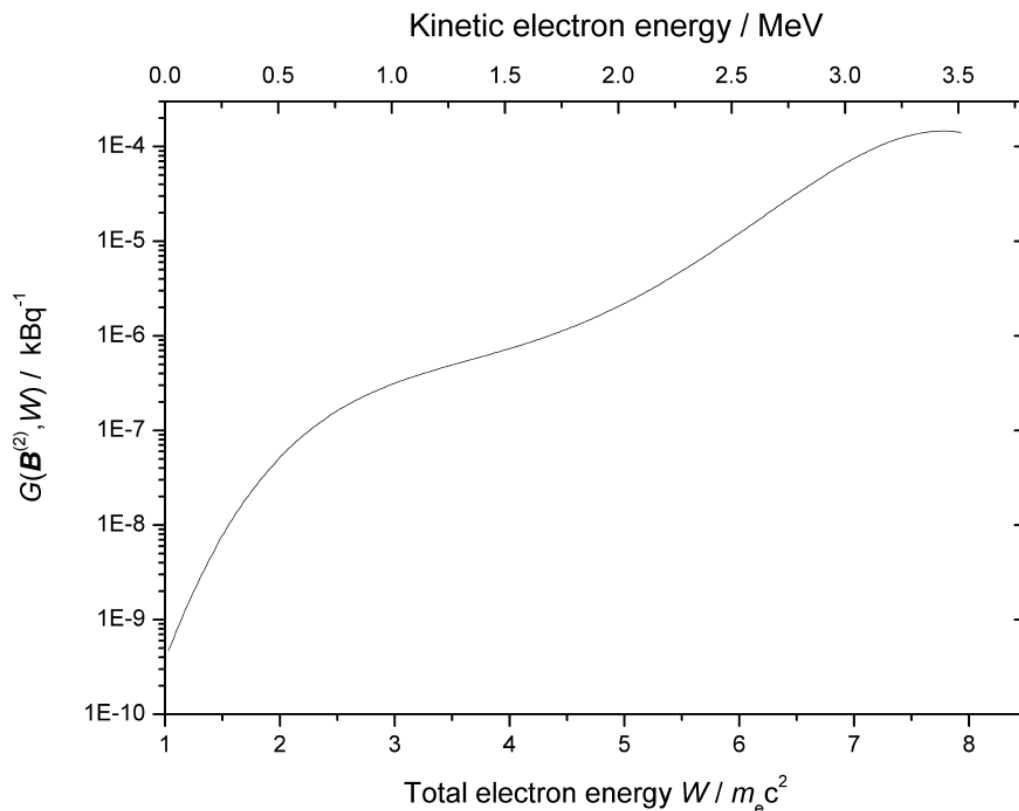


Figure 3 — SIR electron efficiency curve.

The electron efficiency curve (Figure 3, see p. 45) displays a slight decrease at high-energies that is nonphysical. This decrease could be related to the approximate beta spectrum shapes used for non-unique transitions (see Section 11.3 and reference [32], see p. 64).

Figure 4 compares modelled equivalent activity values and measurement results. The reasons for discrepancies between modelled and measured equivalent activities can be problems in the SIR results, in the nuclear data or in the modelled efficiency curves. The larger spread observed in Figure 4 for strong beta emitters (open squares) is related to the lack of SIR data for pure beta emitters, and consequently, the large uncertainty associated with values of the modelled electron efficiency curve. The results for all other radionuclides used in the minimization are in agreement within one or two standard uncertainties.

It is interesting to note that the modelled equivalent activities for ^{103}Ru , ^{85}Sr , ^{134}Cs , ^{137}Cs and ^{95}Nb , which all emit photons mainly between 490keV and 770keV, seem to be slightly overestimated. This systematic behaviour, which was already present in [31], is difficult to understand.

Figure 4 also shows that SIRIC does not reproduce the SIR results for strong β^+ emitters, as expected, due to the extended source effect. Discrepancies observed between the predictions of SIRIC and the measured equivalent activities are discussed below (see also reference [32], see p. 64):

1. For ^{56}Mn , ^{140}Ba and ^{243}Am the problem may come from the measurement results or the nuclear decay data. As there is only a single SIR result for each of these radionuclides, it is difficult to draw a conclusion;

2. The discrepancy observed for ^{65}Zn is due to the nuclear data. Indeed a new SIRIC prediction based on a more recent evaluation of ^{65}Zn decay data [3] is in perfect agreement with the SIR measurement results (circle in Figure 4, see p. 46);
3. The discrepancy for ^{153}Gd is probably due to the nuclear data. This view is supported by the fact that for ^{153}Sm , which presents a similar photon emission, no discrepancy is observed. The efficiency curve therefore provides motivation to investigate the decay data of that radionuclide;
4. For ^{177}Lu the two SIR results available do not agree with each other. The SIRIC prediction is in excellent agreement with one of those results;
5. The case of ^{201}Tl is complex and discussed in reference [32].

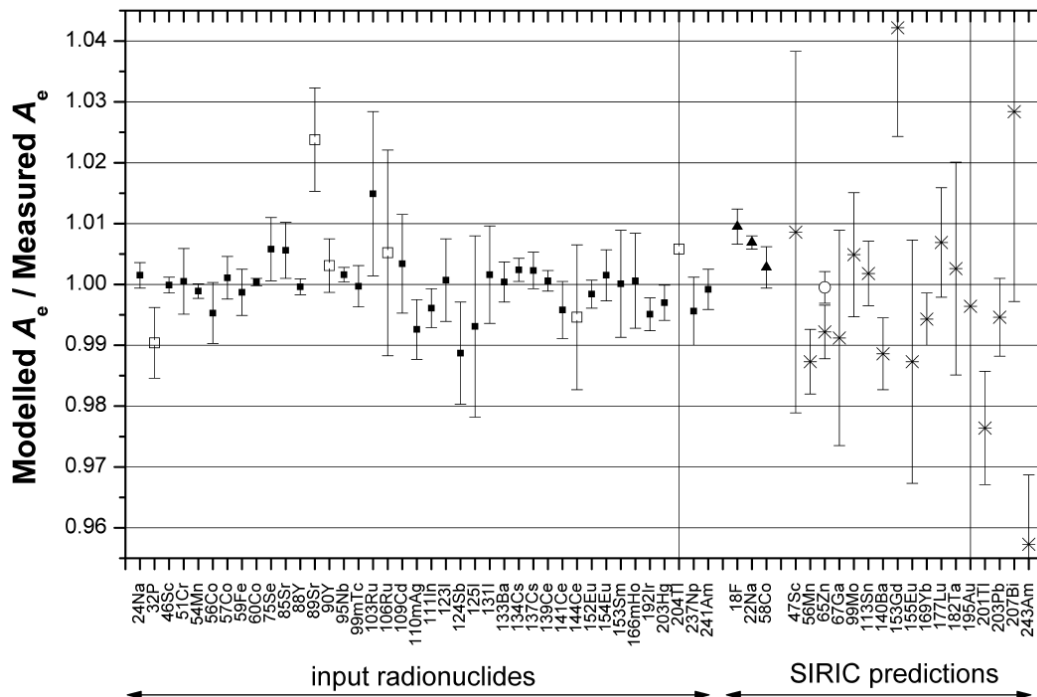


Figure 4 — Comparison of modelled equivalent activity values and measurement results (the KCRV when available). Each bar represents ± 1 standard uncertainty associated with the indicated value at the centre of the bar. Radionuclides used as input to the minimization process are indicated by squares, with (a) open squares denoting pure β emitters or radionuclides with a contribution of the beta emission to the ionization current larger than 15 %, and (b) solid squares denoting the remainder (the bulk) of the radionuclides used as input. Predictions of the SIRIC program for other radionuclides are indicated by asterisks or triangles for strong β^+ emitters. The circle indicates a second prediction for ^{65}Zn using a recent re-evaluation of its decay-scheme parameters.

10.2. Application of the procedure to other ionization chambers

The SIRIC software has also been applied successfully to an ionization chamber similar to that of the SIR, but filled with argon rather than nitrogen. Although the shape of the

photon efficiency curve was very different, particularly at low energy, SIRIC succeeded in reproducing the measurement data using a polynomial of order 8 ([32], and paper in preparation).

This further application demonstrates the flexibility of the software, which is related to the fact that any ionization chamber is expected to show a linear dependence at high photon energy so that the SIRIC model for photon efficiency curve should be appropriate. Nevertheless, tests of SIRIC for various types of ionization chambers would be welcomed. It cannot be excluded that in some cases a different model could enable an adjustment to the data to be made using fewer parameters.

Finally, it has been shown in the literature [22] that ionization chambers with thin outer walls and surrounded by lead shielding may show a discontinuity in the photon efficiency curve at the level of the Pb x-rays K-edge energy. In such a case, the model in SIRIC should be modified but this would have no fundamental consequence on the formulation of the problem to be solved and thus on the procedure applied to find the solution.

11. Conclusions

11.1. Problem formulation

The problem of modelling the photon and electron efficiency curves of an ionization chamber, as part of the SIR (International Reference System for activity measurements of γ -ray emitting radionuclides), has historically been solved using an iterative approach. The approach is iterative in order to deal with the multi-photon emitters. The iteration also relates to adjusting the measured equivalent activities to account for impurities, so that a match can be made with a model depending on the parameters of the efficiency curves by, in turn, adjusting these parameters. In this work, the measured data are not adjusted, but the model itself incorporates the reciprocal of the adjustment. The efficiency curves are expressed empirically, since no physical forms are available. However, they are represented in a way that ensures that whatever the values of the adjustable parameters defining them may be, they remain physically possible (positive and tending to zero at low energy).

11.2. Problem solution

The nature of the formulation means that the efficiency curve parameters can be estimated using a conventional mathematical algorithm for generalized non-linear least-squares minimization, and, moreover, the uncertainty matrix associated with these estimates can be evaluated. However, treating the full formulation of the problem would be computationally prohibitive, since it involves solving not only for the efficiency curve parameters but also for improved estimates of the nuclear data and other quantities. Therefore, a partial formulation is used that can be expected to provide good estimates of the efficiency curve parameters. It is, however, only directly capable of providing estimates of the efficiency curve parameters, and the associated uncertainties that are a consequence of the uncertainties associated with SIR equivalent activity data. Therefore, the law of propagation is applied to the measurement model defined by the generalized non-linear least-squares minimization to obtain the contributions from the uncertainties associated with the nuclear data and other input quantities.

11.3. Scope for further work

The account here does not describe the propagation of the uncertainties associated with the elements of $\hat{\mathbf{K}}$ as their influence is small compared with those of $\hat{\mathbf{D}}$, $\hat{\mathbf{N}}$ and $\hat{\mathbf{R}}$. However, SIRIC actually carries out this propagation although the analysis is not included here.

The emission probabilities $P_{i,j}$ for a given radionuclide i are regarded here as independent. However, SIRIC takes account of the correlation associated with the normalization factor when emission probabilities are expressed in relative terms ($P_{i,j} = \eta_i I_{i,j}$). The real situation is considerably more complicated and in general there will be other appreciable unquantified correlations present. Should information on these correlations be published, the model could be refined to take account of this new data.

It would also be appropriate to consider further correlations that are expected to be present in some cases. Although there is negligible correlation associated with the elements of $\hat{\mathbf{D}}$ for the SIR, correlation effects could be appreciable for a NMI where all primary measured values are obtained using the same method, the same balance, etc. A similar comment applies to correlations associated with the elements of $\hat{\mathbf{D}}$ and $\hat{\mathbf{N}}$, an individual correlation being associated with an element of $\hat{\mathbf{D}}$ and an element of $\hat{\mathbf{N}}$; indeed, an NMI could use nuclear data that it itself measured using the same primary measured values as those included in $\hat{\mathbf{D}}$.

In some cases the use of the beta energy distribution functions (Section 2.3, see p. 17) provided in tabular form may be preferred. In these cases, either the tabular data can be represented by a suitable mathematical function or an appropriate quadrature rule applied to carry out the integration numerically [16] required in evaluating the Equation (11) in Section 3.2.1.

The formulae in appendix B for certain derivatives are implemented using (central) finite-difference formulae. Since this aspect accounts for almost all the computer time required to run the software, replacement of the finite-difference formulae by analytical expressions would give an appreciable improvement in this regard. This aspect would be a useful future development.

The uncertainty calculation described here is complicated, involving applying a generalization of the law of propagation of uncertainty to a vector measurand defined by a generalized non-linear least-squares solution. An implementation of the uncertainty check by Monte Carlo calculation (Section 7.4, see p. 34) would be valuable in validating this aspect of the work.

Appendix 1. Glossary

Symbol	Definition
A	activity of solution at reference date
$A_{i,l}$	measured value for activity of radionuclide i provided by laboratory l
$\hat{A}_{i,l}$	estimate of $A_{i,l}$
A_e	generic equivalent activity (i.e. current-, decay- and impurity-corrected) of solution at reference date
$(A_e)_i$	equivalent activity (i.e. current-, decay- and impurity-corrected) for radionuclide i
$(A_e)_i^{\text{cmptd}}(\mathbf{B}, \mathbf{N})$	computed parameter-dependent equivalent activity (i.e. current-, decay- and impurity-corrected) for radionuclide i given by $(A_e)_i^{\text{cmptd}}(\mathbf{B}, \mathbf{N}) = \theta_i (A_e)_i^{\text{KCRV}} + (1 - \theta_i) (A_e)_i^{\text{model}}(\mathbf{B}, \mathbf{N})$
$(A_e)_{i,l}^{\text{meas}}$	equivalent activity (i.e. current-, decay- and impurity-corrected) corresponding to measured value $A_{i,l}$
$(\hat{A_e})_{i,l}^{\text{meas}}$	estimate of $(A_e)_{i,l}^{\text{meas}}$ equal to $(A_e)_{i,l}^{\text{meas}}(\mathbf{B}^*, \hat{\mathbf{D}}, \hat{\mathbf{N}}, \hat{\mathbf{R}})$
$(A_e)_{i,l}^{\text{meas}}(\mathbf{B}, \hat{\mathbf{D}}, \hat{\mathbf{N}}, \hat{\mathbf{R}})$	quantity-dependent equivalent activity corresponding to measured value $A_{i,l}$
$(A_e)_i^{\text{model}}(\mathbf{B}, \mathbf{N})$	quantity-dependent model value for equivalent activity of radionuclide i
$(\hat{A_e})_i^{\text{model}}$	estimate of $(A_e)_i^{\text{model}}(\mathbf{B}, \mathbf{N})$ equal to $(A_e)_i^{\text{model}}(\mathbf{B}^*, \hat{\mathbf{N}})$
$(A_e)_i^{\text{KCRV}}$	published KCRV for equivalent activity of radionuclide i
\mathbf{B}	column vector $\left((\mathbf{B}^{(1)})^\top, (\mathbf{B}^{(2)})^\top \right)^\top$ of adjustable parameters
$\mathbf{B}^{(1)}$	column vector of adjustable parameters in empirical model for photon efficiency function
$\mathbf{B}^{(2)}$	column vector of adjustable parameters in empirical model for electron efficiency function
$B_h^{(1)}$	element of $\mathbf{B}^{(1)}$
$B_h^{(2)}$	element of $\mathbf{B}^{(2)}$
$\hat{\mathbf{B}}$	prior estimate of \mathbf{B}

\mathbf{B}^*	posterior estimate of \mathbf{B}
$(\mathbf{B}^{(1)})^*$	posterior estimate of $\mathbf{B}^{(1)}$
$(\mathbf{B}^{(2)})^*$	posterior estimate of $\mathbf{B}^{(2)}$
C	generic impurity correction factor
$C_{i,\ell}$	impurity correction factor for radionuclide i and laboratory ℓ
$\hat{C}_{i,\ell}$	estimate of $C_{i,\ell}$
$C_{i,\ell}(\mathbf{B}, \mathbf{N}, \mathbf{R})$	quantity-dependent impurity correction factor for radionuclide i and laboratory ℓ
c	speed of light
D	generic current- and decay-corrected measurement quantity, i.e., equivalent activity not corrected for impurities
\mathbf{D}	vector of the $D_{i,\ell}$ for relevant i, ℓ
$\hat{\mathbf{D}}$	estimate of \mathbf{D}
$D_{i,\ell}$	value of D for radionuclide i and laboratory ℓ
$\widehat{D}_{i,\ell}$	estimate of $D_{i,\ell}$
E	energy of photon
$E_{i,j}$	energy associated with photon j for radionuclide i
E_{\max}	right-hand endpoint of photon energy range over which modelling is carried out
E_{\min}	left-hand endpoint of photon energy range over which modelling is carried out
E_s	s th initial photon energy value
F_s	quotient of ionization currents of radium source numbers 5 and s
$F(\mathbf{B}^{(1)}, E)$	empirical model for photon efficiency function
$f(\mathbf{B}, \mathbf{N}, \mathbf{R})$	equivalent activity model vector given by the vector of the $f_{i,\ell}(\mathbf{B}, \mathbf{N}, \mathbf{R})$ for relevant radionuclides i and laboratories ℓ
$f_{i,\ell}(\mathbf{B}, \mathbf{N}, \mathbf{R})$	so-called equivalent activity model for radionuclide i and laboratory ℓ
$G(\mathbf{B}^{(2)}, E)$	empirical model for electron efficiency function
$H_{i,\ell,k}$	$\exp\left(-(\lambda_k - \lambda_i)\left((t_m)_{i,\ell} - (t_r)_{i,\ell}\right)\right)$, the decay correction applied in the correction for impurities
h	index for model basis functions
$h(\mathbf{B}, \mathbf{D}, \mathbf{N}, \mathbf{R})$	implicit function

$h(\mathbf{Y}, \mathbf{X})$	generic implicit function relating input quantities \mathbf{X} and output quantities \mathbf{Y}
\mathbf{I}	identity matrix
I	set of indices of radionuclides of concern
I	ionization current produced by generic ampoule
$I_{\mathbf{D}}$	subset of indices relating to the vector \mathbf{D} of equivalent activity measurement quantities for the radionuclides and laboratories of concern
I_f	background current
$I_{i,j}$	relative emission probability for j th photon for radionuclide i
$I_{\text{Ra},s}$	ionization current produced by ^{226}Ra source number s , $s = 1, \dots, 5$
i	index for radionuclide
J_i	set of indices of photons associated with radionuclide i
$_{\beta}J_i$	set of indices of beta transitions associated with radionuclide i
j	index for photon or beta transition
j'	index for photon or beta transition
\mathbf{K}	vector of KCRV quantities
$\hat{\mathbf{K}}$	vector estimate of \mathbf{K} (KCRVs) containing the $(A_e)_i^{\text{KCRV}}$
$K_{i,\ell}$	index set for impurities associated with radionuclide i provided by laboratory ℓ
k	index for radionuclide
L_i	set of indices of laboratories that measured radionuclide i
ℓ	index for laboratory
M	generic quantity equal to $F_s \frac{I_{\text{Ra},s} - I_f}{I - I_f} \frac{\exp(-\lambda(t_m - (t_r)))}{\exp(-\lambda_{\text{Ra}}(t_m - t_0))}$
$M_{i,\ell}$	value of M for radionuclide i and laboratory ℓ
$\hat{M}_{i,\ell}$	measured value of $M_{i,\ell}$
M_k	general matrix, $k = 1, 2, \dots$
m	number of actually measured data values
m_e	rest mass of electron
\mathbf{N}	set of quantities constituting the nuclear reference data of which tabulated energies and probabilities $\{E_{i,j} : j \in J_i\}$, $\{P_{i,j} : j \in J_i\}$, $\{W_{i,j} : j \in _{\beta}J_i\}$ and $\{_{\beta}P_{i,j} : j \in _{\beta}J_i\}$ constitute estimates
$\hat{\mathbf{N}}$	prior (tabular) estimate of \mathbf{N}
\mathbf{N}^*	posterior estimate of \mathbf{N}

n	number of basis functions in empirical model for photon efficiency function
n^{\max}	largest value of n to be considered
n_{β}	number of basis functions in empirical model for electron efficiency function
n_{β}^{\max}	largest value of n_{β} to be considered
$P_{i,j}$	emission probability for j th photon for radionuclide i
$_{\beta}P_{i,j}$	emission probability for j th beta transition for radionuclide i
$\mathbf{Q}(\cdot \cdot \cdot)$	orthogonal matrix
$Q_{i,k}(\mathbf{B}, \mathbf{N})$	the quotient $(A_e)_i^{\text{cmptd}}(\mathbf{B}, \mathbf{N}) / (A_e)_k^{\text{cmptd}}(\mathbf{B}, \mathbf{N})$
q	generic number of measurement data
\mathbf{R}	vector of quantities $R_{i,\ell,k}$ for relevant i , ℓ and k
$\hat{\mathbf{R}}$	prior estimate of \mathbf{R}
\mathbf{R}^*	posterior estimate of \mathbf{R}
$R_{i,\ell,k}$	decay-corrected activity of impurity k relative to activity of radionuclide i provided by laboratory ℓ
$\tilde{R}_{i,\ell,k}$	uncorrected counterpart of $R_{i,\ell,k}$
r	generic index
$S_{\text{part}}(\mathbf{B})$	function of adjustable parameters constituting least-squares measure of fit
$S_{\text{full}}(\mathbf{Z})$	full least-squares objective function
$S_{i,j}(\mathbf{W})$	normalized energy distribution function for spectrum corresponding to j th beta transition for radionuclide i
$s(\mathbf{B}, \mathbf{D}, \mathbf{N}, \mathbf{R})$	vector of model deviations $s_{i,\ell}(\mathbf{B}, \mathbf{D}, \mathbf{N}, \mathbf{R})$ arranged according to a prescribed ordering
$s_{i,\ell}(\mathbf{B}, \mathbf{D}, \mathbf{N}, \mathbf{R})$	model deviation for radionuclide i and laboratory ℓ
\mathbf{T}	matrix transpose
$T_h(x)$	Chebyshev polynomial of first kind of degree h (order $h+1$) in x
t_0	fixed SIR reference date
t_m	SIR measurement date
t_r	reference date
$u(\cdot)$	standard uncertainty associated with argument
$u(\cdot, \cdot)$	covariance associated with arguments
$\mathbf{V}(\cdot)$	uncertainty matrix (covariance matrix) associated with argument

$\mathbf{V}^{(k)}(\cdot)$	uncertainty matrix (covariance matrix) associated with argument, $k = 1, 2, \dots$
V_s	screening potential W : total energy of electron
W_c	total energy of conversion electron
$W_{i,j}$	maximum total energy associated with j th beta-transition for radionuclide i
W_{\max}	right-hand endpoint of electron energy range over which modelling is carried out
W_{\min}	left-hand endpoint of electron energy range over which modelling is carried out
\mathbf{X}	generic vector of input quantities
$\hat{\mathbf{X}}$	estimate of \mathbf{X}
x	argument of Chebyshev polynomial
\mathbf{Y}	generic vector of output quantities
$\hat{\mathbf{Y}}$	estimate of \mathbf{Y}
\mathbf{Z}	$(\mathbf{B}^\top, \mathbf{N}^\top)^\top$ or $(\mathbf{B}^\top, \mathbf{N}^\top, \mathbf{R}^\top)^\top$ as appropriate, according to textual context
$\hat{\mathbf{Z}}$	estimate of \mathbf{Z}
\mathbf{Z}^*	posterior estimate of \mathbf{Z}
α	generic element of \mathbf{D} , \mathbf{N} , \mathbf{B} or \mathbf{R} as appropriate, according to textual context
$\boldsymbol{\alpha}$	vector representing \mathbf{N} , \mathbf{D} or \mathbf{R}
ε	generic detection efficiency of ionization chamber
ε_i	detection efficiency of ionization chamber for radionuclide i
$\varepsilon(E)$	efficiency function or curve for ionization chamber for photons of energy E
ε_s	s th efficiency value
$\varepsilon_\beta(W)$	efficiency function or curve for ionization chamber for electrons of energy W
η_i	normalization factor for photon emission probabilities of radionuclide i
θ_i	mixing ratio associated with radionuclide i parameter lying between zero and one
λ_i	decay constant for radionuclide i
λ_n	Coulomb function
λ_{Ra}	decay constant for radionuclide ^{226}Ra

ν	degrees of freedom
$\phi_h(E)$	basis function in empirical model for photon efficiency function
$\psi_h(W)$	basis function in empirical model for electron efficiency function

Appendix 2. Derivatives required by the generalized non-linear least-squares algorithm and in the evaluation of uncertainties

This appendix provides expressions for the derivatives required by the generalized non-linear least-squares algorithm and in the evaluation of uncertainties associated with estimates of the efficiency curve parameters (Section 5.2, see p. 28).

A2.1. Derivatives with respect to decay-corrected measurement quantities

Let α denote any element of \mathbf{D} . Since $f_{i,l}(\mathbf{B}, \mathbf{N}, \mathbf{R})$ does not depend on \mathbf{D} ,

$$\partial f_{i,l}(\mathbf{B}, \mathbf{N}, \mathbf{R}) / \partial \alpha = 0, \text{ all } i, l.$$

From Equation (27) and Equation (22),

$$\frac{\partial s_{i,l}(\mathbf{B}, \mathbf{D}, \mathbf{N}, \mathbf{R})}{\partial \alpha} = \begin{cases} 1 & \alpha \equiv D_{i,l}, \\ 0 & \text{otherwise.} \end{cases} \quad (2.1)$$

A2.2. Derivatives with respect to the remaining quantities

A2.2.1. General

Let α denote any element of \mathbf{B} , \mathbf{N} or \mathbf{R} . From Equation (27),

$$\frac{\partial s_{i,l}(\mathbf{B}, \mathbf{D}, \mathbf{N}, \mathbf{R})}{\partial \alpha} = \frac{\partial f_{i,l}(\mathbf{B}, \mathbf{N}, \mathbf{R})}{\partial \alpha},$$

and hence the derivatives of the model values $f_{i,l}(\mathbf{B}, \mathbf{N}, \mathbf{R})$ are considered. From Equation (22),

$$\begin{aligned} \frac{\partial f_{i,l}(\mathbf{B}, \mathbf{N}, \mathbf{R})}{\partial \alpha} = \frac{1}{C_{i,l}^2(\mathbf{B}, \mathbf{N}, \mathbf{R})} & \left(C_{i,l}(\mathbf{B}, \mathbf{N}, \mathbf{R}) \frac{\partial (A_e)_i^{\text{cmptd}}(\mathbf{B}, \mathbf{N})}{\partial \alpha} \right. \\ & \left. - (A_e)_i^{\text{cmptd}}(\mathbf{B}, \mathbf{N}) \frac{\partial C_{i,l}(\mathbf{B}, \mathbf{N}, \mathbf{R})}{\partial \alpha} \right). \end{aligned} \quad (2.2)$$

From Equation (18) for the correction factor,

$$\frac{\partial C_{i,l}(\mathbf{B}, \mathbf{N}, \mathbf{R})}{\partial \alpha} = \sum_{k \in K_{i,l}} \left[R_{i,l,k} \frac{\partial Q_{i,k}(\mathbf{B}, \mathbf{N})}{\partial \alpha} + Q_{i,k}(\mathbf{B}, \mathbf{N}) \frac{\partial R_{i,l,k}}{\partial \alpha} \right], \quad (2.3)$$

with

$$\frac{\partial Q_{i,k}(\mathbf{B}, \mathbf{N})}{\partial \alpha} = \frac{1}{(A_e)_k^{\text{cmptd}}(\mathbf{B}, \mathbf{N})} \left[\frac{\partial (A_e)_i^{\text{cmptd}}(\mathbf{B}, \mathbf{N})}{\partial \alpha} - Q_{i,k}(\mathbf{B}, \mathbf{N}) \frac{\partial (A_e)_k^{\text{cmptd}}(\mathbf{B}, \mathbf{N})}{\partial \alpha} \right], \quad (2.4)$$

and

$$\frac{\partial R_{i,l,k}}{\partial \alpha} = \begin{cases} 1 & \alpha \equiv R_{i,l,k}, \\ 0 & \text{otherwise.} \end{cases}$$

Then, from Equation (20), since $(A_e)_i^{\text{KCRV}}$ is a constant,

$$\frac{\partial (A_e)_i^{\text{cmptd}}(\mathbf{B}, \mathbf{N})}{\partial \alpha} = (1 - \theta_i) \frac{\partial (A_e)_i^{\text{model}}(\mathbf{B}, \mathbf{N})}{\partial \alpha}. \quad (2.5)$$

Thus, the derivatives $\partial C_{i,l}(\mathbf{B}, \mathbf{N}, \mathbf{R})/\partial \alpha$ are expressed in terms of

1. $Q_{i,k}(\mathbf{B}, \mathbf{N})$, which in turn is expressed in terms of $(A_e)_i^{\text{cmptd}}(\mathbf{B}, \mathbf{N})$,
2. $(A_e)_i^{\text{cmptd}}(\mathbf{B}, \mathbf{N})$, which in turn is expressed in terms of $(A_e)_i^{\text{model}}(\mathbf{B}, \mathbf{N})$,
3. $\partial (A_e)_i^{\text{cmptd}}(\mathbf{B}, \mathbf{N})/\partial \alpha$, which in turn is expressed in terms of $\partial (A_e)_i^{\text{model}}(\mathbf{B}, \mathbf{N})/\partial \alpha$, and
4. \mathbf{R} .

It follows that the provision of $(A_e)_i^{\text{model}}(\mathbf{B}, \mathbf{N})$ and derivatives $\partial (A_e)_i^{\text{model}}(\mathbf{B}, \mathbf{N})/\partial \alpha$ for α corresponding to all particular elements of \mathbf{B} and \mathbf{N} will permit all relevant derivatives to be formed. The following two sections give expressions for the derivatives of $(A_e)_i^{\text{model}}(\mathbf{B}, \mathbf{N})$ with respect to elements of \mathbf{B} , \mathbf{N} and \mathbf{R} , thus, together with Equation (2.1), permitting all derivatives of $s_{i,l}(\mathbf{B}, \mathbf{D}, \mathbf{N}, \mathbf{R})$ with respect to the elements of \mathbf{B} , \mathbf{D} , \mathbf{N} and \mathbf{R} to be determined.

A2.2.2. Derivatives with respect to efficiency curve parameters

From the use of Equation (8),

$$\begin{aligned} \frac{\partial (A_e)_i^{\text{model}}(\mathbf{B}, \mathbf{N})}{\partial B_h^{(1)}} &= -\frac{1}{(A_e)_i^{\text{model}}(\mathbf{B}, \mathbf{N})^2} \sum_{j \in J_i} P_{i,j} \left(\partial F(\mathbf{B}^{(1)}, E_{i,j}) \frac{\partial F(\mathbf{B}^{(1)}, E_{i,j})}{\partial B_h^{(1)}} \right), \\ \frac{\partial (A_e)_i^{\text{model}}(\mathbf{B}, \mathbf{N})}{\partial B_h^{(2)}} &= -\frac{1}{((A_e)_i^{\text{model}}(\mathbf{B}, \mathbf{N}))^2} \sum_{j \in \beta J_i} \beta P_{i,j} \int_i^{W_{i,j}} S_{i,j}(W) \frac{\partial G(\mathbf{B}^{(2)}, W)}{\partial B_h^{(2)}} dW, \end{aligned}$$

where, using Equation (10),

$$\begin{aligned} \frac{\partial F(\mathbf{B}^{(1)}, E)}{\partial B_h^{(1)}} &= \phi_h(\ln E) F(\mathbf{B}^{(1)}, E), \\ \frac{\partial G(\mathbf{B}^{(2)}, W)}{\partial B_h^{(2)}} &= \psi_h(W) G(\mathbf{B}^{(2)}, W). \end{aligned}$$

A2.2.3. Derivatives with respect to nuclear reference data quantities

The use of Equation (8) gives

$$\frac{\partial (A_e)_i^{\text{model}}(\mathbf{B}, \mathbf{N})}{\partial E_{i,j}} = -\frac{1}{P_{i,j} [(A_e)_i^{\text{model}}(\mathbf{B}, \mathbf{N})]^2} \frac{\partial F(\mathbf{B}^{(1)}, E_{i,j})}{\partial E_{i,j}},$$

$$\begin{aligned}\frac{\partial (A_e)_i^{\text{model}}(\mathbf{B}, \mathbf{N})}{\partial P_{i,j}} &= -\frac{1}{[(A_e)_i^{\text{model}}(\mathbf{B}, \mathbf{N})]^2} F(\mathbf{B}^{(1)}, E_{i,j}), \\ \frac{\partial (A_e)_i^{\text{model}}(\mathbf{B}, \mathbf{N})}{\partial W_{i,j}} &= -\beta P_{i,j} S_{i,j}(W_{i,j}) \frac{1}{[(A_e)_i^{\text{model}}(\mathbf{B}, \mathbf{N})]^2} G(\mathbf{B}^{(2)}, W_{i,j}), \\ \frac{\partial (A_e)_i^{\text{model}}(\mathbf{B}, \mathbf{N})}{\partial (\beta P_{i,j})} &= \frac{1}{[(A_e)_i^{\text{model}}(\mathbf{B}, \mathbf{N})]^2} \int_1^{W_{i,j}} S_{i,j}(W) G(\mathbf{B}^{(2)}, W) dW,\end{aligned}$$

where, from Equation (10),

$$\frac{\partial F(\mathbf{B}^{(1)}, E_{i,j})}{\partial E_{i,j}} = F(\mathbf{B}^{(1)}, E_{i,j}) \left(\frac{1}{E_{i,j}} + \sum_{h=1}^n B_h^{(1)} \phi_h'(\ln E_{i,j}) \right).$$

A2.2.4. Derivatives with respect to relative impurity activities

The partial derivatives relating to the relative impurity activities are zero:

$$\frac{\partial (A_e)_i^{\text{model}}(\mathbf{B}, \mathbf{N})}{\partial R_{i,\ell,k}} = 0, \text{ all } i, \ell, k$$

Appendix 3. Hessian matrices

This appendix provides the Hessian matrices, \mathbf{H}_B and the \mathbf{H}_α , required to implement Equation (29). The Hessian matrices require both first derivatives, as given in Appendix 2 in the context of the solution of the generalized non-linear least-squares problem, and second derivatives, as indicated.

Expressions for the matrices \mathbf{H}_B and the \mathbf{H}_α in matrix Equation (29) in terms of s , the vector of model deviations, obtained from Equation (25), are

$$\begin{aligned}\mathbf{H}_B &= \left(\frac{\partial s}{\partial (\mathbf{B})} \right)^\top \mathbf{V}_D^{-1} \frac{\partial s}{\partial \mathbf{B}} + \left(\frac{\partial^2 s}{\partial \mathbf{B}^2} \right)^\top \mathbf{V}_D^{-1} s(\mathbf{B}, \mathbf{D}, \mathbf{N}, \mathbf{R}), \\ \mathbf{H}_D &= \left(\frac{\partial s}{\partial (\mathbf{B})} \right)^\top \mathbf{V}_D^{-1} \frac{\partial s}{\partial \mathbf{D}} + \left(\frac{\partial^2 s}{\partial \mathbf{B} \partial \mathbf{D}} \right)^\top \mathbf{V}_D^{-1} s(\mathbf{B}, \mathbf{D}, \mathbf{N}, \mathbf{R}), \\ \mathbf{H}_N &= \left(\frac{\partial s}{\partial (\mathbf{B})} \right)^\top \mathbf{V}_D^{-1} \frac{\partial s}{\partial \mathbf{N}} + \left(\frac{\partial^2 s}{\partial \mathbf{B} \partial \mathbf{N}} \right)^\top \mathbf{V}_D^{-1} s(\mathbf{B}, \mathbf{D}, \mathbf{N}, \mathbf{R}), \\ \mathbf{H}_R &= \left(\frac{\partial s}{\partial (\mathbf{B})} \right)^\top \mathbf{V}_D^{-1} \frac{\partial s}{\partial \mathbf{R}} + \left(\frac{\partial^2 s}{\partial \mathbf{B} \partial \mathbf{R}} \right)^\top \mathbf{V}_D^{-1} s(\mathbf{B}, \mathbf{D}, \mathbf{N}, \mathbf{R}).\end{aligned}$$

Expressions for the derivatives of the components of s with respect to the components of \mathbf{B} , \mathbf{D} , \mathbf{N} and \mathbf{R} are given in Appendix 2.

The above four formulae are implemented using (central) finite-difference formulae. Also see Section 11.3.

Appendix 4. Implicit multivariate model

Consider the implicit multivariate model

$$h(\mathbf{Y}, \mathbf{X}) = 0,$$

where \mathbf{X} is a vector input quantity comprising mutually independent vector quantities $\mathbf{X}_1, \dots, \mathbf{X}_Q$, i.e. $\mathbf{X} = [\mathbf{X}_1^\top, \dots, \mathbf{X}_Q^\top]^\top$, and \mathbf{Y} a vector output quantity. Suppose that, for $r = 1, \dots, Q$, vector estimates $\hat{\mathbf{X}}_r$ of the \mathbf{X}_r are given, as are the associated uncertainty matrices $\mathbf{V}_{\hat{\mathbf{X}}_r}$. Suppose that the Jacobian matrices

$$\mathbf{J}(\mathbf{X}_r) = \frac{\partial h}{\partial \mathbf{X}_r}, \quad r = 1, \dots, Q,$$

$$\mathbf{J}(\mathbf{Y}) = \frac{\partial h}{\partial \mathbf{Y}}$$

are available. The $\mathbf{J}(\mathbf{X}_r)$ are generally rectangular and $\mathbf{J}(\mathbf{Y})$ is square. An estimate $\hat{\mathbf{Y}}$ of \mathbf{Y} is obtained by solving

$$h(\hat{\mathbf{Y}}, \hat{\mathbf{X}}) = 0, \quad (4.1)$$

and the uncertainty matrix $\mathbf{V}_{\hat{\mathbf{Y}}}$ associated with $\hat{\mathbf{Y}}$ satisfies

$$\mathbf{J}(\hat{\mathbf{Y}}) \mathbf{V}_{\hat{\mathbf{Y}}} \mathbf{J}^\top(\hat{\mathbf{Y}}) = \sum_{r=1}^Q \mathbf{J}(\hat{\mathbf{X}}_r) \mathbf{V}_{\mathbf{X}_r} \mathbf{J}^\top(\hat{\mathbf{X}}_r). \quad (4.2)$$

Since

$$\begin{aligned} \mathbf{V}_{\hat{\mathbf{X}}} &= \text{diag}[\mathbf{V}_{\hat{\mathbf{X}}_1}, \dots, \mathbf{V}_{\hat{\mathbf{X}}_Q}] \\ \mathbf{J}(\mathbf{X}) &= [\mathbf{J}(\mathbf{X}_1), \dots, \mathbf{J}(\mathbf{X}_Q)] \end{aligned}$$

Equation (4.2) can be written as

$$\mathbf{J}(\hat{\mathbf{Y}}) \mathbf{V}_{\hat{\mathbf{Y}}} \mathbf{J}^\top(\hat{\mathbf{Y}}) = \mathbf{J}(\hat{\mathbf{X}}) \mathbf{V}_{\hat{\mathbf{X}}} \mathbf{J}^\top(\hat{\mathbf{X}}),$$

a system that can be solved for $\mathbf{V}_{\hat{\mathbf{Y}}}$.

Using recognized concepts from numerical linear algebra [27], a numerically stable way to form $\mathbf{V}_{\hat{\mathbf{Y}}}$, which accounts for the fact that $\mathbf{J}(\mathbf{X})$ is a rectangular matrix and $\mathbf{J}(\mathbf{Y})$ a square matrix, is as follows [19]:

1. Form the Cholesky factor $\mathbf{U}(\hat{\mathbf{X}})$ of $\mathbf{V}_{\hat{\mathbf{X}}}$. This factor is the upper triangular matrix such that $\mathbf{U}^\top(\hat{\mathbf{X}}) \mathbf{U}(\hat{\mathbf{X}}) = \mathbf{V}_{\hat{\mathbf{X}}}$;
2. Factorize $\mathbf{J}(\hat{\mathbf{Y}})$ as the product $\mathbf{J}(\hat{\mathbf{Y}}) = \mathbf{Q}(\hat{\mathbf{X}}) \tilde{\mathbf{U}}(\hat{\mathbf{X}})$, where $\mathbf{Q}(\hat{\mathbf{X}})$ is an orthogonal matrix and $\tilde{\mathbf{U}}(\hat{\mathbf{X}})$ is upper triangular;

3. Factorize $\mathbf{J}(\hat{\mathbf{Y}})$ as the product $\mathbf{J}(\hat{\mathbf{Y}}) = \mathbf{L}(\hat{\mathbf{Y}})\tilde{\mathbf{U}}(\hat{\mathbf{Y}})$, where $\mathbf{L}(\hat{\mathbf{Y}})$ is lower triangular and $\tilde{\mathbf{U}}(\hat{\mathbf{Y}})$ is upper triangular;
4. Solve the matrix equation $\tilde{\mathbf{U}}^T(\hat{\mathbf{Y}})\mathbf{M}_1 = \mathbf{I}$ for \mathbf{M}_1 ;
5. Solve $\mathbf{L}^T(\hat{\mathbf{Y}})\mathbf{M}_2 = \mathbf{M}_1$ for \mathbf{M}_2 ;
6. Form $\mathbf{M}_3 = \mathbf{Q}^T(\hat{\mathbf{X}})\mathbf{M}_2$;
7. Form $\mathbf{M}_4 = \mathbf{U}^T(\hat{\mathbf{X}})\mathbf{M}_3$;
8. Form $\mathbf{M} = \tilde{\mathbf{U}}(\hat{\mathbf{X}})\mathbf{M}_4$;
9. Orthogonally triangularize \mathbf{M} to give the upper triangular matrix \mathbf{U}^* .
10. Form $\mathbf{V}_{\hat{\mathbf{Y}}} = (\mathbf{U}^{*T}\mathbf{U}^*)$.

This procedure was verified using elementary matrix algebra and tested.

References

- [1] G. Audi and et al. The NUBASE evaluation of nuclear and decay properties. *Nucl. Phys.*, A729:3–128, 2003.
- [2] R. M. Barker, M. G. Cox, A. B. Forbes, and P. M. Harris. SSfM Best Practice Guide No. 4. Discrete modelling and experimental data analysis. Technical report, National Physical Laboratory, Teddington, UK, 2004.
- [3] M.-M. Bé. Activity measurements and determination of gamma-ray emission intensities in the decay of ^{65}Zn . *Appl. Radiat. Isot.*, 64:1396–1402, 2006.
- [4] M.-M. Bé et al. Table of radionuclides. Monographie BIPM-5, Bureau International des Poids et Mesures, Pavillon de Breteuil, F-92312 Sèvres Cedex, France, 2004. <http://www.bipm.org/fr/publications/monographies-ri.html>.
- [5] H. Behrens and J. Jänecke. *Landolt-Börnstein Tables, Gruppe I, Band 4*. Springer, Berlin, 1969.
- [6] BIPM. BIPM Key Comparison Database. www.bipm.org/kcdb.
- [7] BIPM. Mutual recognition of national measurement standards and of calibration and measurement certificates issued by national metrology institutes. International Committee for Weights and Measure, 45 pp., 14 October 1999. Available from the BIPM website: <http://www.bipm.org/pdf/mra.pdf>.
- [8] BIPM, IEC, IFCC, ILAC, ISO, IUPAC, IUPAP, and OIML. Evaluation of measurement data — Supplement 1 to the “Guide to the expression of uncertainty in measurement” — Propagation of distributions using a Monte Carlo method. Joint Committee for Guides in Metrology, Bureau International des Poids et Mesures, JCGM 101, to appear.
- [9] BIPM, IEC, IFCC, ISO, IUPAC, IUPAP, and OIML. Guide to the expression of uncertainty in measurement. International Organisation for Standardisation, Geneva, Switzerland, 1995. ISBN 92-67-10188-9. Corrected and reprinted.
- [10] M. G. Cox. The least squares solution of overdetermined linear equations having band or augmented band structure. *IMA J. Numer. Anal.*, 1:3–22, 1981.
- [11] M. G. Cox. Piecewise Chebyshev series. *Bull. Inst. Math. Appl.*, 22:163–166, 1986.
- [12] M. G. Cox. The NPL Data Approximation Subroutine Library: current and planned facilities. *NAG Newsletter*, 2/87:3–16, 1987.
- [13] M. G. Cox. Survey of numerical methods and metrology applications: discrete processes. In P. Ciarlini, M. G. Cox, R. Monaco, and F. Pavese, editors, *Advanced Mathematical Tools in Metrology*, pages 1–21, Singapore, 1994. World Scientific.
- [14] M. G. Cox. Constructing and solving mathematical models of measurement. In P. Ciarlini, M. G. Cox, F. Pavese, and D. Richter, editors, *Advanced Mathematical Tools in Metrology II*, pages 7–21, Singapore, 1996. World Scientific.
- [15] M. G. Cox. The evaluation of key comparison data. *Metrologia*, 39:589–595, 2002.

- [16] M. G. Cox. The area under a curve specified by measured values. *Metrologia*, 44:365–378, 2007.
- [17] M. G. Cox and P. M. Harris. Software specifications for uncertainty evaluation. Technical Report CMSC 40/04, National Physical Laboratory, Teddington, UK, 2004.
- [18] M. G. Cox and P. M. Harris. SS/M Best Practice Guide No. 6, Uncertainty evaluation. Technical report, National Physical Laboratory, Teddington, UK, 2004.
- [19] M. G. Cox and P. M. Harris. SS/M Best Practice Guide No. 6, Uncertainty evaluation. Technical Report DEM-ES-011, National Physical Laboratory, Teddington, UK, 2006.
- [20] M. G. Cox, P. M. Harris, P. D. Kenward, and Emma Woolliams. Spectral characteristic modelling. Technical Report CMSC 27/03, National Physical Laboratory, Teddington, UK, 2003.
- [21] M. G. Cox, P. M. Harris, and Emma R. Woolliams. Data evaluation of key comparisons involving linked bilateral measurements and multiple artefacts. In *NCSL International Workshop and Symposium*, Washington, USA, 2005.
- [22] A. de Vismes and M.-N. Amiot. Towards absolute activity measurements by ionisation chambers using the penelope monte-carlo code. *Appl. Radiat. and Isot.*, 59:267–272, 2003.
- [23] P. Dryák and L. Dvořák. Measurement of the energy response functions of the ÚVVVR and SIR $4\pi\gamma$ ionization chambers. *Appl. Radiat. Isot.*, 37:1071–1073, 1986.
- [24] B. Ford, J. Bentley, J. J. du Croz, and S. J. Hague. The NAG Library ‘machine’. *Software – Practice and Experience*, 9:56–72, 1979.
- [25] CEA/LNHB (France), PTB (Germany), INEEL (USA), KRI (Russia), LBNL (USA), NPL (UK), and CIEMAT (Spain). DDEP, Decay Data Evaluation Project, 2004. <http://www.nucleide.org/DDEP.htm>.
- [26] P. E. Gill, W. Murray, and M. H. Wright. *Practical Optimization*. Academic Press, London, 1981.
- [27] G. H. Golub and C. F. Van Loan. *Matrix Computations*. John Hopkins University Press, Baltimore, MD, USA, 1996. Third edition.
- [28] A. Grau Malonda. Free parameter models in liquid scintillation counting. In *Colección Documentos Ciemat*, Madrid, 1999.
- [29] K. V. Mardia, J. T. Kent, and J. M. Bibby. *Multivariate Analysis*. Academic Press, London, 1979.
- [30] C. Michotte. Influence of radioactive impurities on SIR measurements. *Appl. Radiat. Isot.*, 52:319–323, 2000.
- [31] C. Michotte. Efficiency curve of the ionization chamber of the SIR. *Appl. Radiat. Isot.*, 56:15–20, 2002.

- [32] C. Michotte, A. K. Pearce, M. G. Cox, and J.-J. Gostely. An approach based on the SIR measurement model for determining ionization chamber efficiency curves, and a study of ^{65}Zn and ^{201}Tl photon emission intensities. *Appl. Radiat. and Isot.*, 64:1147–1155, 2006.
- [33] C. Michotte and G. Ratel. Key comparison results and the determination of the KCRV, CCRI(II)/03-28. Technical report, BIPM, 2003. [http://www.bipm.org/cc/CCRI\(II\)/Allowed/17/CCRI\(II\)03-28.pdf](http://www.bipm.org/cc/CCRI(II)/Allowed/17/CCRI(II)03-28.pdf).
- [34] L. Nielsen. Identification and handling of discrepant measurements in key comparisons. Technical Report DFM-02-R28, Danish Institute of Fundamental Metrology, Denmark, 2002.
- [35] National Nuclear Data Center. ENSDF, Evaluated Nuclear Structure Data File, 2004.
- [36] A. K. Pearce, C. Michotte, and Y. Hino. Ionization chamber efficiency curves. *Metrologia*, 44:S67–S70, 2007.
- [37] G. Ratel and C. Michotte. BIPM comparison BIPM.RI(II)-K1.Yb-169 of activity measurements of the radionuclide ^{169}Yb and links for the 1997 regional comparison EUROMET.RI(II)-K2.Yb-169. *Metrologia*, 41:06017, 2004.
- [38] D. F. G. Reher, M. J. Woods, B. R. S. Simpson, and G. Ratel. Portability of the calibration of SIR of BIPM to other ionization chambers for radioactivity measurements. *Appl. Radiat. Isot.*, 49:1417–1419, 1998.
- [39] M. E. Rose. *Phys. Rev. Lett.*, 49:727–729, 1936.
- [40] A. Rytz. The international reference system for activity measurements of γ -ray emitting nuclides. *Appl. Radiat. Isot.*, 34:1047–1056, 1983.
- [41] H. Schrader. Activity measurements with ionization chambers. Monographie BIPM-4, Bureau International des Poids et Mesures, Pavillon de Breteuil, F-92312 Sèvres Cedex, France, 1997.
- [42] H. Schrader. Calibration and consistency of results of an ionization-chamber secondary standard measuring system for activity. *Appl. Radiat. Isot.*, 52:325–334, 2000.
- [43] H. Schrader and A. Švec. Comparison of ionization chamber efficiencies for activity measurements. *Appl. Radiat. Isot.*, 60:369–378, 2004.
- [44] A. Švec and H. Schrader. Fitting methods for constructing energy-dependent efficiency curves and their application to ionization chamber measurements. *Appl. Radiat. Isot.*, 56:237–243, 2002.
- [45] D. H. Wilkinson. Evaluation of beta-decay. Part I. The traditional phase space factors. *Nucl. Instrum. Methods Phys. Res.*, A275:378–386, 1989.
- [46] D. H. Wilkinson. Evaluation of beta-decay. Part II. Finite mass and size effects. *Nucl. Instrum. Methods Phys. Res.*, A290:509–515, 1990.

- [47] D. H. Wilkinson. Evaluation of beta-decay. Part V. The Z-independent outer radiative corrections for allowed decay. *Nucl. Instrum. Methods Phys. Res.*, A365:497–507, 1995.
- [48] D. H. Wilkinson. Evaluation of beta-decay. Part VI. The Z-dependent outer radiative corrections for allowed decay. *Nucl. Instrum. Methods Phys. Res.*, A401:275–280, 1997.
- [49] D. H. Wilkinson. Evaluation of beta-decay. Part VII. The Z-independent outer radiative corrections for unique-forbidden decay. *Nucl. Instrum. Methods Phys. Res.*, A406:89–92, 1998.



